UNIVERSIDADE FEDERAL DE ALFENAS

ANDRÉ TEIXEIRA DA SILVA HUCKE

IMPACTOS DAS MUDANÇAS CLIMÁTICAS NAS PRINCIPAIS BACIAS DO BRASIL: ANÁLISE COMPARATIVA ENTRE MODELOS HIDROLÓGICOS E MODELOS DE INTELIGÊNCIA ARTIFICIAL

POÇOS DE CALDAS/MG

2023

ANDRÉ TEIXEIRA DA SILVA HUCKE

IMPACTOS DAS MUDANÇAS CLIMÁTICAS NAS PRINCIPAIS BACIAS DO BRASIL: ANÁLISE COMPARATIVA ENTRE MODELOS HIDROLÓGICOS E MODELOS DE INTELIGÊNCIA ARTIFICIAL

Dissertação apresentada como parte dos requisitos do para obtenção do título de Mestre em Ciência e Engenharia Ambiental pela Universidade Federal de Alfenas. Área de concentração: Recursos hídricos.

Prof. Orientador: Dr. Rafael de Oliveira Tiezzi

POÇOS DE CALDAS/MG

2023

Sistema de Bibliotecas da Universidade Federal de Alfenas
Biblioteca Campus Poços de Caldas

Hucke, André Teixeira da Silva.
Impactos das mudanças climáticas nas principais bacias do Brasil : Análise comparativa entre modelos hidrológicos e modelos de inteligência artificial / André Teixeira da Silva Hucke. - Poços de Caldas, MG, 2023.
82 f. : il. -

Orientador(a): Rafael de Oliveira Tiezzi.
Dissertação (Mestrado em Ciência e Engenharia Ambiental) - Universidade Federal de Alfenas, Poços de Caldas, MG, 2023.
Bibliografia.

1. Inteligência Artifical. 2. Mudanças climáticas. 3. Impactos ambientais. 4. Energia elétricfa. 5. Recursos hídricos. I. Tiezzi, Rafael de Oliveira, orient. II. Título.

Ficha gerada automaticamente com dados fornecidos pelo autor.

ANDRÉ TEIXEIRA DA SILVA HUCKE

“Impactos das mudanças climáticas nas principais bacias do Brasil: Análise comparativa entre modelos hidrológicos e modelos de inteligência artificial”

O Presidente da banca examinadora abaixo assina a aprovação da Dissertação apresentada como parte dos requisitos para a obtenção do título de Mestre em Ciência e Engenharia Ambiental pela Universidade Federal de Alfenas. Área de concentração: Recursos Hídricos

Aprovada em: 04 de julho de 2023.

Prof. Dr. Rafael de Oliveira Tiezzi

Presidente da Banca Examinadora

Instituição: Universidade Federal de São Carlos

Prof. Dr. Paulo Sergio Franco Barbosa

Instituição: Universidade de Campinas

Prof. Dr. Flavio Aparecido Gonçalves

Instituição: Universidade Federal de Alfenas

A minha mãe e pai, por sempre mostrar novos caminhos e perspectivas. To my newfound family, always keen to help. To my Toya, the sunshine of my life. I am eternally grateful.

AGRADECIMENTOS

Agradeço ao meu orientador, por estar sempre disposto e sempre me dar espaço para novos testes e ideias que surgiram durante o mestrado. Também agradeço ao Mateus Nardini Menegaz, por sua incrível ajuda com dados e conversas esclarecedoras.

O presente trabalho foi realizado com apoio da Coordenação de Aperfeiçoamento de Pessoal de Nível Superior - Brasil (CAPES) - Código de Financiamento 001.

RESUMO

O Brasil alcançou o maior índice de produção energética a partir de fontes renováveis, principalmente hidrelétrica, que demanda manejo correto das águas dos reservatórios para manter o mesmo nível de produção. A energia elétrica e o Produto Interno Bruto (PIB) estão intrinsecamente conectados e fica evidente a importância do Sistema Interligado Nacional (SIN) para a integração de diferentes fontes de geração de energia elétrica, redução de custos de investimento e aumento da segurança e confiabilidade do sistema. Para tal, o manejo correto dos recursos hídricos, ferramentas preditivas e planejamento estratégico para a exploração de novas usinas hidrelétricas torna-se imprescindível. Por meio de modelagem de diferentes cenários climáticos e uso de inteligência artificial propõe-se avaliar os impactos das mudanças climáticas nos sistemas hidrelétricos.

Palavras-chave: mudanças climáticas; energia hidráulica; projeção pluviométrica; planejamento energético.

ABSTRACT

Brazil has achieved the highest index of energy production from renewable sources, mainly hydroelectric, which requires proper management of reservoir water to maintain the same level of production. Electric power and Gross Domestic Product (GDP) are intrinsically connected, and the importance of the National Interconnected System (SIN) for integrating different sources of electricity generation, reducing investment costs, and increasing system security and reliability becomes evident. To achieve this, proper management of water resources, predictive tools, and strategic planning for the development of new hydroelectric power plants are essential. By modeling different climate scenarios and utilizing artificial intelligence, it is proposed to assess the impacts of climate change on hydroelectric systems.

Keywords: climate change; hydropower; rainfall projection; energy planning.

LISTA DE FIGURAS

LISTA DE TABELAS

Artigo I

Artigo II

LISTA DE SIGLAS

ALPA	Alto Paranapanema Basin
ANA	Agência Nacional de Águas
ANN	Artificial Neural Network
ANOVA	Analysis of Variance
AR	Assessment Report
CESM	Community Earth System Model
CNN	Convolutional Neural Networks
DGM	Modelo de Água Subterrânea de Darcy
GCM	Community Earth System Model
IA	Inteligência Artificial
INPE	Instituto Nacional de Pesquisas Espaciais
IPCC	Intergovernmental Panel on Climate Change
LSTM	Long Short-Term Memory
LSM	Linear Stochastic Model
MME	Ministério de Minas e Energia
NSE	Nash-Sutcliffe Model Efficiency Coefficient
ONS	Operador Nacional de Sistemas
PBIAS	Percent Bias
PIB	Produto Interno Bruto
RPC	Representative Concentration Pathways
RMSE	Root Mean Squared Error
RSR	RMSE-Observations Standard Deviation Rate
RHM	Regional Hydrologic Model
RNN	Recurrent Neural Networks
SMAP	Soil Moisture Accounting Procedure
SIN	Sistema Interligado Nacional
SSARR	Streamflow Synthesis and Reservoir Regulation
SVM	Support Vector Machines
UMAP	Uniform Manifold Approximation and Projection

SUMÁRIO

1 INTRODUÇÃO

Em 2023 o Brasil atingiu o maior índice de produção energética a partir de fontes renováveis. Essas fontes incluem eólica, solar e, em maior parte, hidráulica. Para manter esse mesmo nível de produção, o manejo correto das águas que abastecem as usinas hidráulicas é fundamental e tem ganhado mais força frente às mudanças climáticas. Além do manejo correto para a produção de energia, também é necessário considerar outros usos das águas em reservatórios em todo o território nacional. As regiões do Nordeste brasileiro são caracterizadas por escassez de água, enquanto outras regiões, como o Centro-Oeste e Norte, apresentam maiores índices pluviométricos. Porém, mesmo em regiões com mais chuvas, ainda podem ocorrer eventos mínimos extremos como entre os anos de 2014, 2016 e 2021, onde uma prolongada seca afetou os níveis dos reservatórios da região Sudeste e colocou o sistema energético e de abastecimento de água da região sob estresse.

Na figura 1 está apresentada a produção de energia hidrelétrica mundial. Nessa figura, vemos que o Brasil é o terceiro maior produtor de energia elétrica através de recursos hídricos, produzindo cerca de 285 TWh. Além disso, o Brasil possui uma das maiores reservas naturais de recursos hídricos. O manejo desse recurso finito torna-se imprescindível e, para tal, o conhecimento entre relação entre o clima e a disponibilidade de água precisa ser aprofundado.

Figura 1 - Produção mundial de usinas hidrelétricas por país

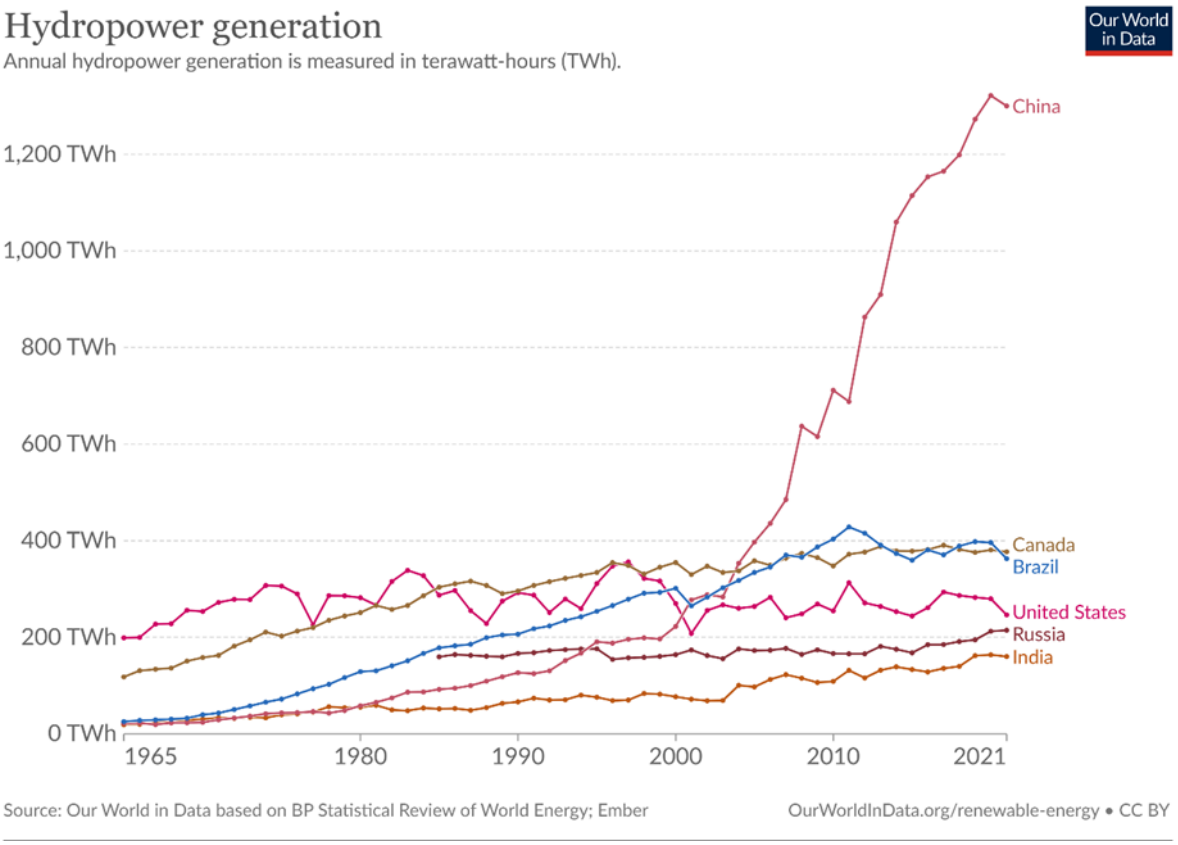

Fonte: Adaptado de Our World in Data (2023).

Quando se trata de manejo dos recursos hídricos, o Brasil tem dois caminhos disponíveis. O primeiro seria manejar os reservatórios já existentes para que eles continuem produzindo energia e abastecendo cidades ao seu redor. O segundo caminho é o manejo para novas usinas, já que o Brasil ainda possui capacidade de expansão das usinas hidrelétricas. Em torno de 40% dos recursos hídricos ainda têm potencial teórico de exploração e o planejamento estratégico correto para o futuro dessas usinas é importante (MME, 2020).

Sempre existiu uma relação entre PIB e demanda energética. Segundo o Ministério de Minas e Energia, no ano de 2021 o PIB nacional cresceu mais que a demanda energética em apenas 0,1% (MME, 2020). As fontes renováveis, que representam 85% da matriz energética, compõem 44,7% da energia total gerada pelo Brasil, incluindo transporte e indústria. Porém, as usinas hidrelétricas foram afetadas pela falta de chuva e enfatizam a necessidade de um bom manejo dos recursos hídricos e ferramentas que auxiliem os gestores de bacias hidrográficas a predizer as relações entre clima e volume nos reservatórios.

O Sistema Interligado Nacional (SIN) é um complexo sistema de energia elétrica que interconecta as redes elétricas de todo o Brasil. É um sistema de grande importância para o país, pois permite a integração da geração de energia elétrica de diferentes fontes e regiões,

além de garantir a segurança e confiabilidade do suprimento de energia elétrica para os consumidores.

Segundo o MME, o SIN é constituído por um conjunto de instalações e equipamentos de geração, transmissão e distribuição de energia elétrica, que são interligados por meio de linhas de transmissão e subestações. O MME também afirma que o SIN é dividido em quatro subsistemas: Sul, Sudeste/Centro-Oeste, Nordeste e Norte.

Segundo Mercedes, Rico e Pozzo (2015), uma importância atual do SIN é a integração de fontes renováveis de energia na matriz energética brasileira e permite a integração de diferentes fontes de geração de energia elétrica, o que aumenta a segurança e a confiabilidade do sistema e reduz os custos de investimento. De acordo com o artigo, o SIN possui uma capacidade de transmissão de energia elétrica de mais de 70.000 MW, o que permite a integração da energia gerada por usinas hidrelétricas, termelétricas e eólicas.

Para o planejamento do SIN é importante a utilização de ferramentas hidrológicas para o cálculo de vazões. Com isso, é possível prever a quantidade de água retida nos reservatórios. Os modelos usuais de análise se baseiam em planilhas de Excel e, com o renovado potencial de inteligência artificial, poderiam ficar desatualizadas frente a essa nova ferramenta que agora tem a capacidade computacional suficiente para aprender dezenas de milhares de parâmetros.

A inteligência artificial (IA) é um campo da ciência da computação que se concentra no desenvolvimento de algoritmos e sistemas capazes de simular habilidades humanas como percepção, raciocínio, aprendizagem e tomada de decisões.

Esses sistemas podem ser projetados para executar tarefas específicas, como reconhecimento de voz ou imagem, tradução de idiomas ou análise de dados, além de serem capazes de aprender com os dados e melhorar seu desempenho ao longo do tempo.

A IA é uma tecnologia em constante evolução, com aplicações em diversas áreas, como saúde, finanças, transportes, segurança, entre outras. A expectativa é que a IA continue a avançar rapidamente, oferecendo novas oportunidades e desafios para a sociedade.

A previsão do tempo é uma das tarefas mais importantes e desafiadoras na meteorologia. Nos últimos anos, a IA tem sido cada vez mais utilizada para aprimorar a precisão das previsões do tempo. Vários estudos têm explorado o uso de técnicas de aprendizado de máquina, como redes neurais artificiais, árvores de decisão e algoritmos genéticos, para prever o clima com maior precisão.

1.1 OBJETIVOS

1.1.1 Objetivos Gerais

Aqui propomos dois objetivos. **O primeiro objetivo do estudo é avaliar os possíveis impactos das mudanças** climáticas nos reservatórios Jurumirim e Chavantes e os possíveis conflitos gerados pela escassez hídrica. **O segundo objetivo é comparar ferramentas** normalmente utilizadas pelo Operador Nacional do Sistemas Elétricos (ONS) e hidrológicos, conhecidos como SMAP e MEL, com modelos de rede neural, conhecidos como CNN e RNN, para a predição de vazões para 25 das principais bacias hidrográficas do Brasil. Para tal, foram utilizados dados obtidos do CPTEC/INPE que prevê chuvas futuras para os próximos 100 anos em diferentes modelos globais regionalizados. Ambas as redes neurais e os modelos convencionais foram calibrados e validados com dados reais de chuva e evapotranspiração, obtidos do ONS. Para a padronização dos resultados, utilizou-se modelagem calculadas pelo SMAP para os mesmos anos históricos disponíveis, de 1960 a 1990.

2 DESENVOLVIMENTO

2.1 Recursos Hídricos e Geração de Energia Elétrica

Os recursos hídricos são fontes essenciais para a geração de energia elétrica em diversas partes do mundo. A energia hidrelétrica é uma fonte renovável e limpa que tem sido amplamente utilizada para atender às necessidades de eletricidade em muitos países.

Um estudo recente de Lobo *et al*. (2023), analisou o uso da modelagem numérica para prever o comportamento do fluxo de água em reservatórios de hidrelétricas. Através da aplicação de técnicas de modelagem avançadas, os pesquisadores conseguiram prever a distribuição do fluxo de água em diferentes pontos do reservatório. Este estudo é importante porque pode ajudar a otimizar o uso dos recursos hídricos para a geração de energia elétrica, maximizando a eficiência das hidrelétricas.

Além disso, pesquisas têm sido realizadas para avaliar a viabilidade de outras fontes de energia renovável, como a energia das ondas do mar. Segundo Silva (2021) os resultados mostraram que a energia das ondas do mar pode ser uma fonte viável de energia renovável, especialmente em áreas com altas ondas do mar.

Outra área importante de pesquisa em recursos hídricos é a gestão da água para a produção de energia elétrica. Um estudo de Maraschin *et al*. (2022) avaliou a importância da gestão integrada da água e da energia em bacias hidrográficas. Os resultados mostraram que a gestão integrada da água e da energia pode melhorar a eficiência do uso dos recursos hídricos para a produção de energia elétrica.

2.2 Modelos Climatológicos

2.2.1 Modelos Climáticos Globais

Os modelos climáticos globais são ferramentas essenciais para a compreensão do clima terrestre e suas mudanças ao longo do tempo. Eles utilizam informações sobre a atmosfera, os oceanos, a superfície terrestre e outros fatores para simular as condições climáticas presentes e futuras.

Um artigo publicado por Taylor *et al*. (2012) destaca a importância dos modelos climáticos globais para a previsão de mudanças climáticas futuras e para a elaboração de políticas públicas que buscam mitigar seus efeitos. Os autores ressaltam que esses modelos

são cada vez mais precisos e sofisticados, mas ainda apresentam desafios, como a representação adequada de processos físicos complexos e a dificuldade em lidar com a variabilidade climática natural.

Outro estudo, conduzido por Flato *et al*. (2013), apresenta uma revisão detalhada dos modelos climáticos globais e suas aplicações. Os autores discutem a importância de considerar fatores como as emissões de gases de efeito estufa, a mudança no uso da terra e a poluição do ar na elaboração dos modelos. Eles também enfatizam a necessidade de continuar aprimorando essas ferramentas, a fim de aumentar sua precisão e confiabilidade.

Um exemplo de modelo climático global é o Community Earth System Model (CESM), desenvolvido por Hurrell *et al*. (2013). O CESM incorpora informações sobre a atmosfera, os oceanos, a criosfera (regiões cobertas por gelo e neve) e a biologia terrestre, permitindo a simulação de uma ampla gama de processos climáticos. O modelo tem sido utilizado em diversos estudos sobre mudanças climáticas e seus impactos, como o estudo de Fasullo, Otto-Bliesneri e Stevenson (2018) sobre a intensificação de secas em regiões dos Estados Unidos.

2.2.2 Modelos Climáticos Regionais

Os modelos climáticos regionais são ferramentas importantes para prever as mudanças climáticas em escalas regionais. Esses modelos utilizam dados observacionais, como temperatura, pressão atmosférica, umidade e vento, para simular o clima em uma determinada região.

Segundo o estudo de Reboita *et al*. (2018), os modelos climáticos regionais têm melhor desempenho do que os modelos globais em prever mudanças climáticas regionais. Isso se deve ao fato de que os modelos regionais levam em consideração a topografia e a influência do oceano, enquanto os modelos globais tratam a Terra como uma superfície plana.

Além disso, de acordo com o estudo de Pal *et al*. (2019), os modelos climáticos regionais são capazes de fornecer informações mais detalhadas sobre eventos climáticos extremos, como ondas de calor e chuvas intensas, em comparação com os modelos globais. Isso é especialmente importante para regiões onde esses eventos têm impacto na população e na economia local.

No entanto, é importante ressaltar que os modelos climáticos regionais ainda têm limitações, principalmente devido à falta de dados observacionais em algumas regiões.

Segundo o estudo de Christensen *et al*. (2007), a qualidade dos resultados dos modelos depende da qualidade e quantidade dos dados utilizados como entrada.

2.3 Modelos Hidrológicos

Os modelos hidrológicos são ferramentas importantes para a previsão de eventos hidrológicos, como enchentes e secas, e para o gerenciamento de recursos hídricos. Eles usam princípios físicos, químicos e matemáticos para simular o comportamento dos sistemas hidrológicos e fornecer previsões.

Um exemplo de modelo hidrológico amplamente utilizado é o Modelo de Água Subterrânea de Darcy (DGM), que foi desenvolvido por Henry Darcy (1856). Ele descreve a velocidade e a direção do fluxo de água subterrânea em um meio poroso e permeável, com base na Lei de Darcy.

Outro modelo hidrológico popular é o Modelo de Chuva-Vazão, que usa dados de precipitação e informações topográficas para simular o fluxo de água em uma bacia hidrográfica. Um exemplo de modelo de chuva-vazão é o Modelo Hidrológico de Dados Distribuídos (Distributed Hydrological Model, DHSVM), que foi desenvolvido por Wigmosta, Vail e Lettenmaier (1994).

O Modelo de Bacia Hidrográfica IV de Stanford descrito por Crawford e Linsley (1966) é outro modelo amplamente utilizado na área da hidrologia. Este modelo foi um dos esforços pioneiros no campo da modelagem hidrológica digital que utiliza computadores para simular o movimento da água através de uma bacia hidrográfica. O modelo incorporava equações matemáticas e algoritmos para representar os processos físicos envolvidos na hidrologia, contendo vários componentes e suas interconexões. O modelo lida com dados de entrada, como padrões de chuva, características do solo e informações de uso da terra, que resulta em simulação para comparar dados observados, e a precisão e confiabilidade do modelo são avaliadas.

Outro modelo descrito no artigo produzido por Hyung-san (2016) é o Streamflow Synthesis and Reservoir Regulation (SSARR). O modelo hidrológico é usado para simular o fluxo de água em uma bacia hidrográfica e para otimizar a operação de reservatórios. O modelo é amplamente utilizado na engenharia de recursos hídricos para auxiliar na gestão de sistemas hídricos complexos, como bacias hidrográficas ou sistemas de reservatórios. O SSARR também pode ser usado para avaliar o impacto de mudanças climáticas na disponibilidade de água e para realizar análises de sensibilidade e otimização da operação dos

sistemas de reservatórios. Ele fornece informações essenciais para tomada de decisões relacionadas à gestão integrada de recursos hídricos, permitindo a otimização dos recursos hídricos disponíveis.

Além disso, os modelos hidrológicos são frequentemente utilizados em conjunto com modelos climáticos para prever o impacto das mudanças climáticas nos recursos hídricos. Um exemplo de modelo hidrológico acoplado ao clima é o Modelo Hidrológico Regional (Regional Hydrologic Model, RHM), que foi desenvolvido por Wood *et al*. (2004).

2.3.1 Modelos Determinísticos

Entre os diferentes tipos de modelos hidrológicos, o Soil Moisture Accounting Procedure (SMAP) é uma abordagem amplamente utilizada para estimar a umidade do solo e a disponibilidade de água para as plantas.

O SMAP é um modelo hidrológico simples que usa equações de balanço de água para estimar a umidade do solo e a disponibilidade de água para as plantas. O modelo leva em consideração as entradas de água (precipitação, infiltração e irrigação), as saídas de água (evaporação, transpiração e escoamento superficial) e as mudanças de armazenamento de água no solo.

O SMAP é amplamente utilizado em estudos hidrológicos e de gestão de recursos hídricos. Por exemplo, em um estudo realizado por Campos, Santos e Assis (2018), o SMAP foi usado para avaliar o impacto das mudanças no uso do solo na disponibilidade de água em uma bacia hidrográfica no rio Almada no Brasil. O estudo mostrou que apesar de diferentes níveis de antropoformização, a disponibilidade de água não é afetada e se mantém similar ao longo de toda a bacia hidrográfica.

Outro estudo realizado por de Fernandes *et al*. (2016) usou o SMAP para avaliar o impacto das mudanças climáticas na disponibilidade de água em uma bacia hidrográfica na bacia de Orós, Ceará. O estudo mostrou que as mudanças climáticas na maioria dos modelos analisados afetaram negativamente em até 62.1% a disponibilidade de água na bacia hidrográfica e um deslocamento sazonal das chuvas, devido ao aumento da evapotranspiração causada pelo aumento da temperatura.

2.3.2 Modelos Estocásticos

Dentre as diversas abordagens existentes, o modelo estocástico linear é um dos mais utilizados. Este modelo é baseado na teoria dos processos estocásticos, e considera que a série temporal de uma variável hidrológica pode ser decomposta em um componente determinístico e um componente estocástico.

Um exemplo de aplicação do modelo estocástico foi realizado por Wang *et al*. (2021), que utilizaram este modelo para analisar a variabilidade da vazão. Os resultados obtidos indicaram que o modelo estocástico foi capaz de capturar as principais características da série temporal de vazão do rio.

Outro exemplo de aplicação do modelo estocástico linear foi realizado por Câmara *et al*. (2016), que utilizaram este modelo para prever a vazão do Rio Tocantins, no Brasil. Os resultados obtidos indicaram que o modelo estocástico linear pode ser utilizado na previsão de vazão em curto prazo, e que este modelo pode ser uma ferramenta auxiliar viável para a previsão de vazão em sistemas hidrológicos complexos.

Além disso, a aplicação do modelo estocástico também tem sido utilizada em estudos de mudanças climáticas. Um exemplo foi realizado por Abdelaziz *et al*. (2023), que utilizaram este modelo para analisar o impacto das mudanças climáticas na vazão do Rio Nilo, no Egito. Os resultados indicaram que o modelo estocástico linear pode ser uma ferramenta útil para avaliar os efeitos das mudanças climáticas na disponibilidade hídrica de uma bacia hidrográfica, sendo uma forma simples que não requer grandes quantidades de recursos computacionais.

2.3.3 Modelos de Inteligência Artificial

Um dos estudos mais recentes na área de previsão do tempo com uso de IA foi conduzido por Sabino (2019). Neste estudo, os autores propuseram uma abordagem baseada em redes neurais profundas para prever a temperatura máxima diária. Eles utilizaram dados de temperatura, pressão atmosférica, umidade relativa e velocidade do vento coletados em uma estação meteorológica para treinar o modelo de rede neural. Os resultados mostraram que a abordagem proposta superou outras técnicas de previsão de temperatura, como imagem por satélite e regressão linear múltipla. Além disso, apresentou alta precisão na previsão da temperatura máxima diária.

Outro estudo interessante na área de previsão do tempo com uso de IA foi conduzido por Prasad e Kumar

(2021). Neste estudo, os autores propuseram uma abordagem baseada em árvores de decisão para prever a precipitação diária. Eles utilizaram dados de temperatura, umidade relativa, velocidade do vento, pressão atmosférica e dados de radar para treinar o modelo de árvore de decisão. Os resultados mostraram que a abordagem proposta superou outras técnicas de previsão de precipitação e apresentou alta precisão na previsão da precipitação diária.

Além disso, um estudo de Gill, Singh e Singh (2010) explorou o uso de algoritmos genéticos para otimizar modelos de previsão do tempo baseados em redes neurais artificiais. Os resultados mostraram que o modelo otimizado apresentou alta precisão na previsão da temperatura, umidade relativa e velocidade do vento.

2.4 Mudanças Climáticas e Matriz Energética

2.4.1 Mudanças Climáticas

As mudanças climáticas são um dos maiores desafios enfrentados pela humanidade no século XXI, e a matriz energética é uma das principais responsáveis por essas mudanças. O uso de combustíveis fósseis como carvão, petróleo e gás natural é uma das principais causas do aumento das emissões de gases de efeito estufa na atmosfera, o que leva a um aumento da temperatura média do planeta e alterações no clima global.

Um dos principais desafios na transição para uma matriz energética mais limpa e renovável é a redução das emissões de gases de efeito estufa. De acordo com o relatório especial do Painel Intergovernamental sobre Mudanças Climáticas (IPCC) de 2018 sobre o aquecimento global de 1,5°C, é necessário reduzir as emissões globais de gases de efeito estufa em cerca de 45% em relação aos níveis de 2010 até 2030, e atingir emissões líquidas zero até cerca de 2050, para limitar o aquecimento global a 1,5°C acima dos níveis pré-industriais.

A transição para uma matriz energética mais limpa e renovável pode envolver uma combinação de medidas, incluindo a implantação de energias renováveis, como solar, eólica, hidroelétrica, geotérmica e biomassa, e a adoção de tecnologias de armazenamento de energia e eficiência energética. Além disso, a transição para uma matriz energética mais limpa pode trazer benefícios econômicos, sociais e ambientais, como a criação de empregos, redução da poluição do ar e da água e melhorias na segurança energética.

Um estudo publicado por Jacobson *et al*. (2021) analisou as implicações de uma transição global para uma matriz energética 100% renovável até 2050, em comparação com um cenário de referência que continuaria a depender dos combustíveis fósseis. Os autores concluíram que a transição para uma matriz energética 100% renovável seria economicamente viável e teria impactos positivos na saúde humana, na redução das emissões de gases de efeito estufa e na segurança energética.

Outro estudo, realizado por Lima *et al*. (2020), avaliou a contribuição das energias renováveis na redução das emissões de gases de efeito estufa no Brasil. Os autores concluíram que a implantação de energias renováveis no país poderia reduzir as emissões de gases de efeito estufa em cerca de 32% até 2030, em comparação com o cenário de referência.

2.4.2 Cenários Futuros

Segundo Williams *et al*. (2021), os cenários futuros indicam uma tendência de aumento das temperaturas globais, com consequências para a intensidade e frequência de eventos climáticos extremos, como secas, tempestades e ondas de calor. Adicionalmente, as mudanças climáticas têm impactos nos ecossistemas terrestres e aquáticos, além de alterar a distribuição geográfica de diversas espécies.

Para lidar com essa situação, é necessário promover uma mudança na matriz energética, reduzindo a dependência de combustíveis fósseis e investindo em fontes renováveis, como a solar, a eólica e a hidráulica. O avanço da tecnologia e o aumento da eficiência energética também são importantes para garantir uma transição suave e sustentável.

O IPCC é a principal organização internacional responsável pela avaliação científica das mudanças climáticas e seus impactos, e emitiu vários relatórios importantes ao longo dos anos.

O mais recente relatório do IPCC**, o** Assessment Report 6 (AR6), publicado em 2021, conclui que as mudanças climáticas estão ocorrendo em todo o mundo a uma taxa sem precedentes e que as ações humanas são a principal causa dessas mudanças. O relatório também destaca a importância da redução das emissões de gases de efeito estufa para limitar os impactos das mudanças climáticas.

Um estudo recente da UNESCO (2021) aponta que os investimentos em fontes renováveis de energia superaram os de combustíveis fósseis pelo terceiro ano consecutivo, impulsionados principalmente pela China e pelos países da União Europeia. O relatório

também destaca a importância de políticas públicas e regulamentações que incentivem a transição para fontes limpas de energia.

Uma maneira importante de reduzir as emissões de gases de efeito estufa é através da transição para uma matriz energética mais limpa e renovável. Por exemplo, um estudo de Almeida, Paiva e Muniz (2017), menciona que a energia renovável poderia fornecer até 86% da demanda global de energia até 2050.

No entanto, a transição para uma matriz energética mais limpa e renovável enfrenta vários desafios, incluindo questões regulatórias, tecnológicas e financeiras. É necessário um esforço coordenado e colaborativo entre governos, setor privado e sociedade civil para superar esses desafios e alcançar uma transição bem-sucedida para uma matriz energética mais limpa e sustentável.

2.4.3 Impactos

Um estudo publicado por Stocker *et al*. (2013) mostra que as mudanças climáticas estão afetando a saúde humana em todo o mundo, aumentando o risco de doenças respiratórias, cardiovasculares e infecciosas. Além disso, as mudanças climáticas têm impactos nos ecossistemas, com o aumento da frequência e intensidade de eventos climáticos extremos, como secas, tempestades e ondas de calor, o que pode levar à perda de biodiversidade e destruição de habitats naturais (IPCC, 2018).

Para mudar a matriz energética e promover fontes de energia limpas e renováveis, é necessário investir em tecnologias e infraestrutura adequadas. De acordo com um estudo publicado por Creutzig *et al*. (2017), o uso de fontes de energia renováveis pode reduzir as emissões de gases de efeito estufa, mas é necessário implementar políticas públicas que incentivem a transição para uma matriz energética limpa.

Um exemplo de política pública que tem se mostrado eficaz é o estabelecimento de metas de redução de emissões de gases de efeito estufa, como as metas estabelecidas pelo Acordo de Paris. Um estudo de Schmidt *et al*. (2018) mostrou que o cumprimento das metas estabelecidas pelo Acordo de Paris pode reduzir os impactos das mudanças climáticas, incluindo a redução da frequência e intensidade de eventos climáticos extremos.

Impactos incluem o aumento do nível do mar. As mudanças climáticas estão causando o derretimento das geleiras e calotas polares, o que está contribuindo para o aumento do nível do mar em todo o mundo. Um estudo publicado por Church *et al*. (2013) mostrou que o nível médio global do mar aumentou cerca de 19 centímetros desde 1901.

Outro impacto são as alterações nos padrões de precipitação. As mudanças climáticas também estão afetando os padrões de precipitação em todo o mundo, aumentando a frequência e intensidade de eventos climáticos extremos, como inundações e secas. Um estudo publicado por Sheffield e Wood (2008) mostrou que a frequência de secas graves e prolongadas aumentou em todo o mundo nas últimas décadas.

Entre os muitos outros impactos, mais um impacto notável são ameaças à segurança alimentar e morte de espécies polinizadoras. As mudanças climáticas também estão afetando a produção agrícola em todo o mundo, ameaçando a segurança alimentar de milhões de pessoas. Um estudo publicado por Lobell *et al*. (2011) mostrou que as mudanças climáticas estão reduzindo a produtividade das safras em todo o mundo, especialmente em regiões tropicais e subtropicais.

2.4.4 Mitigação dos Impactos

A principal estratégia para mitigar os impactos das mudanças climáticas é reduzir as emissões de gases de efeito estufa. Isso pode ser feito através de políticas e tecnologias que promovem a eficiência energética, o uso de energias renováveis e a captura e armazenamento de carbono. No entanto, a implementação dessas estratégias enfrenta desafios políticos, econômicos e tecnológicos.

Outra estratégia importante é a adaptação às mudanças climáticas já em curso, por meio do desenvolvimento de infraestrutura resistente a eventos climáticos extremos, sistemas de alerta precoce e medidas de gestão de recursos naturais. No entanto, a adaptação enfrenta desafios de financiamento e coordenação entre diferentes setores e níveis de governança.

Por fim, a redução da vulnerabilidade social é crucial para garantir que as comunidades mais afetadas pelas mudanças climáticas tenham acesso a recursos e serviços essenciais, como água potável, serviços de saúde e segurança alimentar. Isso requer ações políticas que abordem as desigualdades socioeconômicas e promovam o acesso equitativo a serviços e recursos.

O governo pode oferecer subsídios para incentivar a adoção de energias renováveis, tornando-as mais competitivas em relação aos combustíveis fósseis. Isso pode incluir incentivos fiscais, financiamento para pesquisa e desenvolvimento, e outras medidas para promover o crescimento do setor de energia renovável.

Também é possível implementar políticas para limitar as emissões de gases de efeito estufa, como impostos sobre carbono, padrões de eficiência energética para veículos e edifícios, e limites de emissão para as indústrias.

Outra forma seria fornecer financiamento para a pesquisa e desenvolvimento de tecnologias limpas, como energia solar, eólica e armazenamento de energia, bem como tecnologias para a captura e armazenamento de carbono.

2.5 Resultados Esperados

O trabalho está estruturado na forma de dois artigos. Para o primeiro artigo, o objetivo é obter uma perspectiva das possíveis tendências da vazão para dois importantes reservatórios, Jurumirim e Chavantes. Com essa informação, busca-se entender quais são as fragilidades e conflitos em torno do uso de água na região. Para tal, será realizado uma avaliação de diferentes modelos climatológicos e cenários.

Para o segundo artigo, o objetivo é obter uma rede neural que possa complementar o escopo de ferramentas dos hidrólogos e gestores de bacias hidrográficas. Os mesmos modelos e cenários serão aplicados, mas agora com foco em 25 das principais bacias hidrográficas do Brasil. Desta forma será realizada a construção de dois modelos de inteligência artificial baseados nas duas arquiteturas mais conhecidas do campo. A análise constituirá uma avaliação entre períodos de normais climatológicas, em busca de entender se os modelos convencionais usados pelos hidrólogos e os modelos de inteligência artificial convergem nas predições.

2.6 Artigo I: Predictive Modeling for Improved Water Resource Management in the Alto Paranapanema Basin

Andre T. S Hucke[1]
Mateus Menegaz[2]
Jorge Isidoro[3]
Rafael de Oliveira Tiezzi[4 *]

Abstract

Climate change is a reality that changes the landscape. With the application of predictive modeling techniques to improve water resource management in the Alto Paranapanema Basin, it is possible to plan ahead and mitigate some of the impacts and water conflicts, being a region with over 1600 agriculture pivots. Through the use of a physical model known as Soil Moisture Accounting Procedure (SMAP), long-term climate datasets and river flow are simulated. Global Climate Models (GCMs) downscaled with the Eta model provide future climate scenarios based on Representative Concentration Pathways (RCPs). The results indicate a temporal displacement of rainfall, with a decrease during the wet season and an increase during the dry season. These changes pose challenges for water availability, hydroelectric power generation, and agriculture. Collaboration between basin management units and the utilization of predictive models can support proactive water resource management strategies to mitigate the effects of climate change and ensure sustainable water allocation in the Alto Paranapanema Basin.

Keywords: *Soil Moisture Accounting Procedure, Climate Change, Representative Concentration Pathways, Predictions, Modeling*

1 INTRODUCTION

[1] [1, 2] Institute of Science and Technology, Federal University of Alfenas, Rodovia José Aurélio Vilela, 11999 (BR 267 Km 533), Cidade Universitária, Poços de Caldas, MG CEP 37715-400, Brazil. andre.hucke@sou-unifal.mg.edu.br. matmenegaz@hotmail.com.
[3] University of Algarve. jorge.mgp.isidoro@gmail.com
[4] Institute of Science and Technology, Federal University of Alfenas, Rodovia José Aurélio Vilela, 11999 (BR 267 Km 533), Cidade Universitária, Poços de Caldas, MG CEP 37715-400, Brazil. rafaeltiezzi@ufscar.br
* Corresponding Author: rafaeltiezzi@ufscar.br

The latest AR6 published by the IPCC in August 2021 unequivocally asserts that human influence is responsible for the faster pace of climate change, exceeding what would occur naturally. The report confirms that greenhouse gasses emitted from human activities are the main culprit (IPCC, 2021). The impacts of climate change are widespread and diverse, ranging from rising sea levels and altered rainfall patterns to changes in evapotranspiration and energy supply in nations heavily reliant on hydroelectric power. In addition, climate change poses a significant threat to food security (Zhang *et al*., 2018).

The relationship between humans and climate prediction dates back to the origin of agriculture, which marked the first large-scale food supply for humanity and was essential for population growth and technological development (Commoner, 2020). However, the planet already faces significant disruptions to its ecosystems, and there is a limit to the maximum population the world can sustain. In the early days of agriculture, people viewed the seasons as milestones to determine when to plant different crops and how long food stores would last. Currently, this concept of carefully observing climate behavior is more relevant than ever, as human activity is heavily dependent on water resources, and climate change is altering the spatial and temporal distribution of rainfall. While modern climate prediction requires advanced supercomputers, it remains as essential as it was for our ancestors (Jackson *et al*., 2001).

The complexity of climate, including its multiple factors that influence weather patterns and climate change, makes accurate prediction remarkably difficult (Gueymard, 2012). However, statistical models offer a means of predicting climate trends by analyzing historical data, despite inherent uncertainties. One useful tool for climate prediction is the stochastic climate generator, which can simulate hydrological series based on historical data. To assess the effectiveness of such simulations, several common methods are employed to determine the degree of statistical correlation with historical data, such as the Nash-Sutcliffe model efficiency coefficient (NSE).

Global Climate Models (GCMs) are computer simulations used to predict how the climate will respond to future changes (Chou *et al*., 2014). The outputs of GCMs can be incorporated as inputs to stochastic models, which can generate projections based on the IPCC Representative Concentration Pathways (RCPs), indicating how much greenhouse gas emissions are expected to increase (van Vuuren *et al*., 2011). GCMs are generated and provided by several institutions, including the Canadian Centre for Climate Modelling and Analysis, the Center for Climate System Research, the National Institute of Space Research

(INEP), and the Met Office Hadley Centre. To improve their accuracy, GCMs can also be downscaled or regionalized by incorporating additional variables, such as topography, land use, or local climate data that are specific to the region under analysis. In Brazil, the regionalization process is performed by INEP, which uses multiple GCMs to better represent and understand possible future climate scenarios in Brazil (Chou *et al*., 2014).

Simulating long-term climate datasets for a specific region and altering its initial conditions is a feasible approach to understand the impact of climate change on future rainfall, evapotranspiration, and river flow (Green *et al*., 2011; Maraun *et al.*, 2010). To this end, in Brazil, hydrologists widely employ the Soil Moisture Accounting Procedure (SMAP), which utilizes rainfall and evapotranspiration data to derive river flow. The SMAP model generates both unit runoff values, a measure of the watershed's water production per unit area, and total river flow discharge (Barros *et al*., 2009). Further details on SMAP can be found in Lopes, Braga and Conejo (1982).

The relationship between rainfall and runoff is not linear and depends on specific watershed characteristics, such as land use and basin slope. The interconnection between different sub-basins of watersheds has a significant influence on the river flow downstream, as the runoff from upstream watersheds affects the river flow in downstream watersheds. This phenomenon is known as incremental watersheds. Although headwater watersheds are located miles away upstream, they can significantly impact the quantity and quality of water downstream along the river path (Skaggs, Brevé and Gilliam, 1994).

In Brazil, one of the major headwater watersheds for hydroelectric generation is in the State of São Paulo and is known as the Alto Paranapanema Basin (ALPA). The Rio Paranapanema basin, in which the ALPA is the headwater sub basin, has 11 hydroelectric power plants located in this basin with a total output of 2,4 GW (SIRGH, 2016). This basin is also one of the tributaries of the Parana River, that leads to the Itaipu dam, the second biggest hydroelectric power plant in the world regarding installed capacity (14 GW). Another major feature of this basin is its agricultural potential.

ALPA sub basin has the highest pivot count of all sub basins in the State of Sao Paulo, with an aggressive increase through the years, as shown in Figure 1, with more than 1600 in 2017. Because of the amount of agriculture pivots, the ALPA sub basin region has the biggest GDP in the State of Sao Paulo. In this State, the agriculture sector corresponds to 14% of its GDP, divided in 20% to livestock and 80% to farms (Barros *et al.*, 2021). In 2022, the State of Sao Paulo was responsible for around 25% of Brazil’s GDP (IBGE, 2023).

Figure 1 – Increase in agriculture pivots on the ALPA region between 1985, with 3 agriculture pivots, and 2017, with over 1600 agriculture pivots

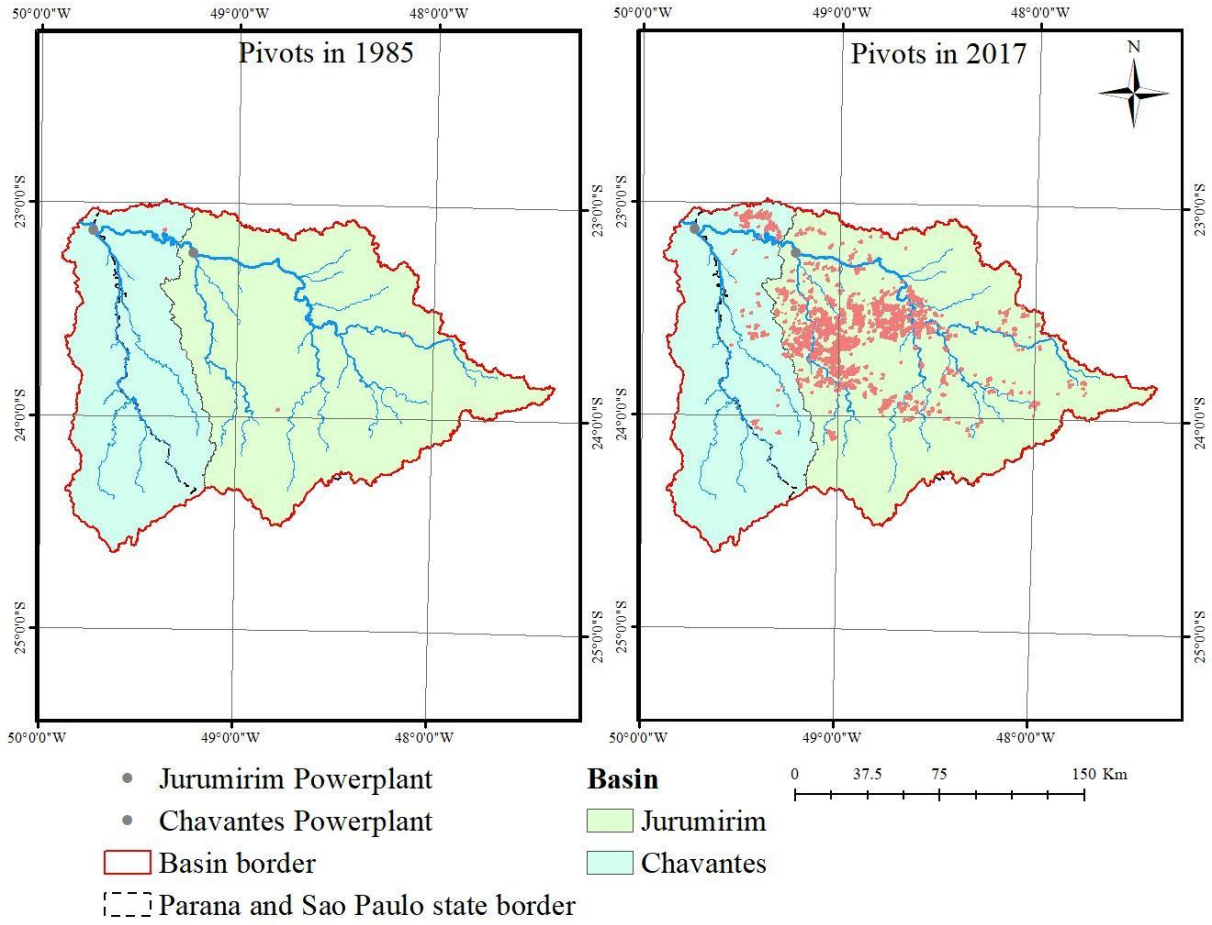

Source: ANA (2019).

The aim of this study was to investigate the potential impacts of climate change on rainfall and river flow in two key watersheds, Jurumirim and Chanvantes. These watersheds play a critical role in supplying water to the Avare region's cities, and are also important for the local economy, including tourism and property values around the reservoir. Climate change can significantly alter hydrologic processes in the watersheds, which in turn can affect communities along the river, disrupt electricity generation in hydroelectric plants, and impact agriculture and livestock practices in the region. Furthermore, these changes can have a ripple effect throughout all connected rivers. Despite the abundance of research on the impacts of climate change on hydrological systems, few studies have incorporated such a large number of climate models and scenarios for basins with such a significant impact on society, as is the case in this study.

2 METHOD

2.1 Basin Characteristics

The methodology adopted for this study was based on previous research carried out in the Alto Paranapanema basin (ALPA) (Tiezzi *et al*., 2018 and Tiezzi *et al*., 2019). The ALPA basin covers an area of 22,689 km², with an average elevation of 610 meters, and is home to major industrial, agricultural, and livestock sites. However, according to SIGRH (2023), only 4,677 km² of the area was still covered by natural forests in 2023, and this is unfortunately expected to continue diminishing. The basin spans across the São Paulo and Paraná State limits, as depicted in Figure 2. To analyze the impacts of climate change in the region, the basin was divided into two sub-basins, with the first sub-basin's pour point located in the Jurumirim reservoir and the second sub-basin's pour point located in the Chavantes reservoir. Rainfall data generated by ETA/INEP, containing all GCM components, was used for all the counties within the basin (Chou *et al*., 2014).

Chavantes power plant has a production capacity of 414 MW and a reservoir area of 428.34 km². Jurumirim power plant has a production capacity of 100.96 MW and a reservoir of 449 km². It is worth noting that the water flowing through this basin comes from the Paranapanema River and the Itararé River, and it plays a crucial role in regulating water resources in the region.

Figure 2 - Localization of Alto do Paranapanema basin (ALPA), in the State of Sao Paulo, in Brazil with further details on ALPA

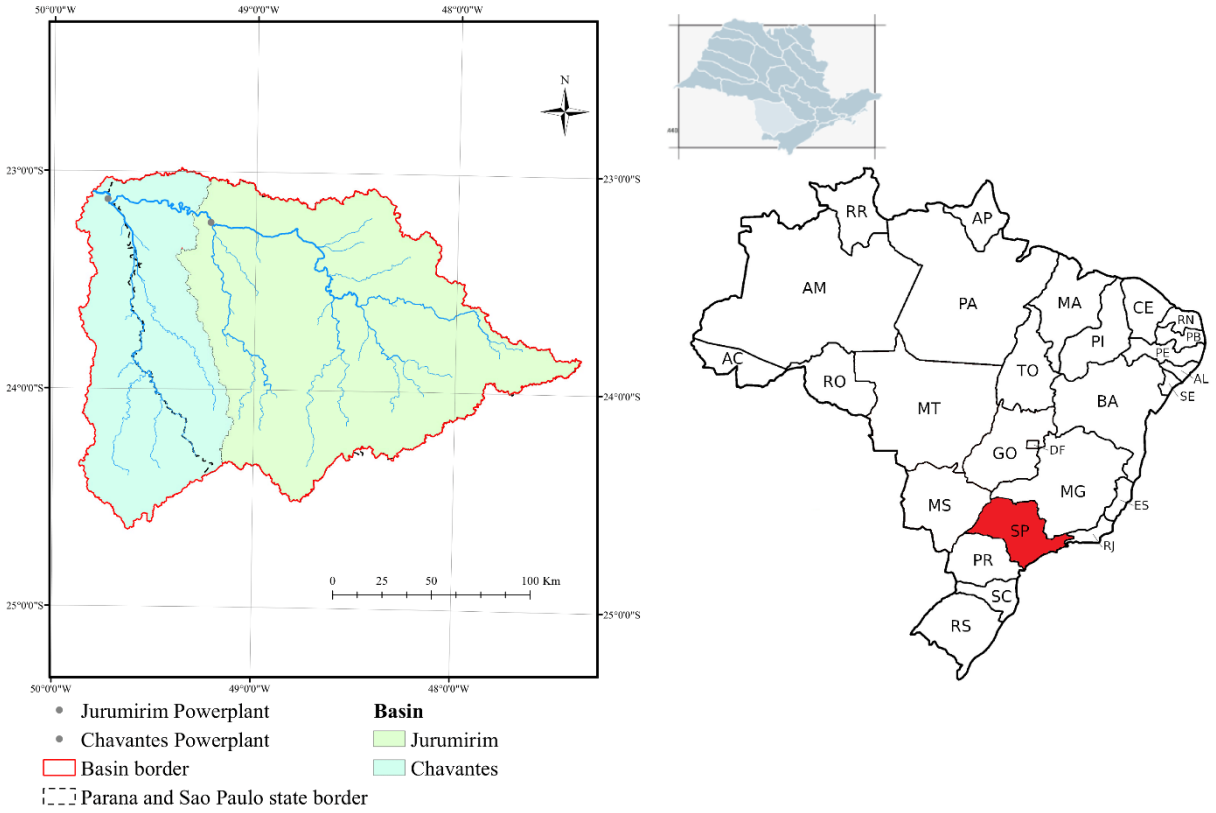

Source: Adapted from SigRH (2023).

To simulate how the GCMs will represent the climate and optimize the time it takes to do such simulations, the GCMs are first modeled by several different institutions. The grid size for these models typically ranges from 400 × 400 km to 200 × 200 km. The regional climate models (RCM), like the Eta model, takes the GCM and focuses computational efforts to improve the output data (Chou *et al*., 2014). Table 1 summarizes some GCM models and their main features.

Table 1 - GCMs models and its characteristics. Source: Author.

Model	Institution	Resolution (latº x longº)	Levels	Vegetation	Addition information
BESM	National Institute for Space Research, Brazil	0.25º to 2º × 1º	28 terrestrial and 50 oceanic	12 different types	Radioactive interactions and convective cloud system
	Canadian Center for	2.8125º ×	35	9	Carbon cycle

CanESM2	Climate Modeling and Analysis, Canada	2.8125º	atmospheric	different types in 3 different vegetative systems	components and dead organic matter
HadGEM2-EM	Met Office Hadley Center, United Kingdom	1.875º × 1.25º	38 atmospheric	5 different types	Model with atmospheric chemistry with aerosols
Miroc5	Japan Agency for Marine-Earth Science and Technology, Atmosphere and Ocean Research Institute, Japan	1.41º × 1.41º	40 terrestrial and 50 oceanic	3 groups	Uses albedo of snow and water mirrors. Also uses clouds microphysics

The ETA model has been adapted to facilitate downscaling, which involves regionalizing global models on a more precise scale that is tailored to the Central and South American regions. It has been utilized by CPTEC/INPE for meteorological forecasts since 1997. Starting from 2010, this model was also employed for studying climate change driven by global models. Eta incorporates annual dynamics of the microphysical vegetation cycle of clouds, a convective cloud scheme, and short- and long-wave balance at a constant CO_2 concentration (Chou *et al*., 2014).

These GCMs (see Table 1) were selected as these were the only four GCMs regionalized using the Eta model. After coupling these models, certain modifications were made, resulting in four variants: Eta-BESM, Eta-CanESM, Eta-HadGEM2-ES, and Eta-Miroc5. Precipitation and evapotranspiration data spanning the period from 1960 to 1989, as well as projections up to 2100 based on RCPs, were obtained using these models. The Eta model employs a vertical resolution of 38 levels and a spatial resolution of 20 km (Chou *et al*., 2014). It is important to clarify that although the Eta models generate a significant amount of data, only precipitation and evapotranspiration were considered for modeling the rainfall-to-river flow process in this study.

Only the RCP 4.5 and 8.5 scenarios were employed for the different regionalized Eta models, as they represent the best and worst-case scenarios projected by the IPCC. The RCP 2.6 scenario was excluded from this study since its predictions are expected to occur soon, and the main aim of this paper is to investigate the potential impacts if the scenarios worsen. Similarly, the RCP 6.0 scenario was not used to focus solely on the extremes and simplify the analysis.

To enhance the accuracy of the models employed in this study, a meticulous calibration process was undertaken using historical data obtained from reputable sources such

as the National Water Agency (ANA) and the National System Operator (ONS). Typically, historical series spanning a period of 5 to 10 years were utilized to convert rainfall into runoff or flow through the application of a model. In this study, the Soil Moisture Accounting Procedure (SMAP) model was specifically adopted, which has been extensively utilized in previous research and has undergone validation in multiple studies (Barros *et al*., 2009; O'Neill *et al*., 2010; Peng *et al*., 2021; Wigneron *et al*., 2017; Zhang and Zhou, 2016). The SMAP model operates by calculating flow based on precipitation and evaporation and is classified as a concentrated parametric model. To optimize the model's performance, the Nash-Sutcliffe coefficient was selected as the optimization criterion, employing Excel's SOLVER (Nash & Sutcliffe, 1970).

3 RESULTS AND DISCUSSION

The dimensionless average monthly rainfall for the RCP 4.5 and 8.5 scenarios, as well as the four different regional climate models, from 2010 to 2099 are presented in Figure 2. The dimensionless average is represented as a percentage, with values above the 100% mark indicating increases and values below indicating reductions. The results were obtained by comparing the calculated rainfall against the historical rainfall data from ALPA. Most models indicate a decrease in rainfall from December to April, and an increase in rainfall from May to July. However, for the other months from August to November, there is no clear signal when comparing the different models. It is worth noting that the Eta-BESM model is considered the best representative model for the Alto Paranapanema region (Chou *et al*., 2014), as it indicates a shift in rainfall throughout the year. Specifically, this model shows that the dry months experience an increase in rainfall, whereas the wet months have a potential increase in extreme rainfall events. Overall, the dry months become even drier, while the wet months may become more extreme.

Figure 3 – Nondimensional average of monthly rainfall and evapotranspiration for ALPA, in comparison to historical rainfall, over the period of 2010 to 2099. The results are based on four different climate models: Eta-BESM, Eta-CanESM, Eta-HadGEM, and Eta-Miroc, and two IPCC scenarios: RCP 4.5 and 8.5

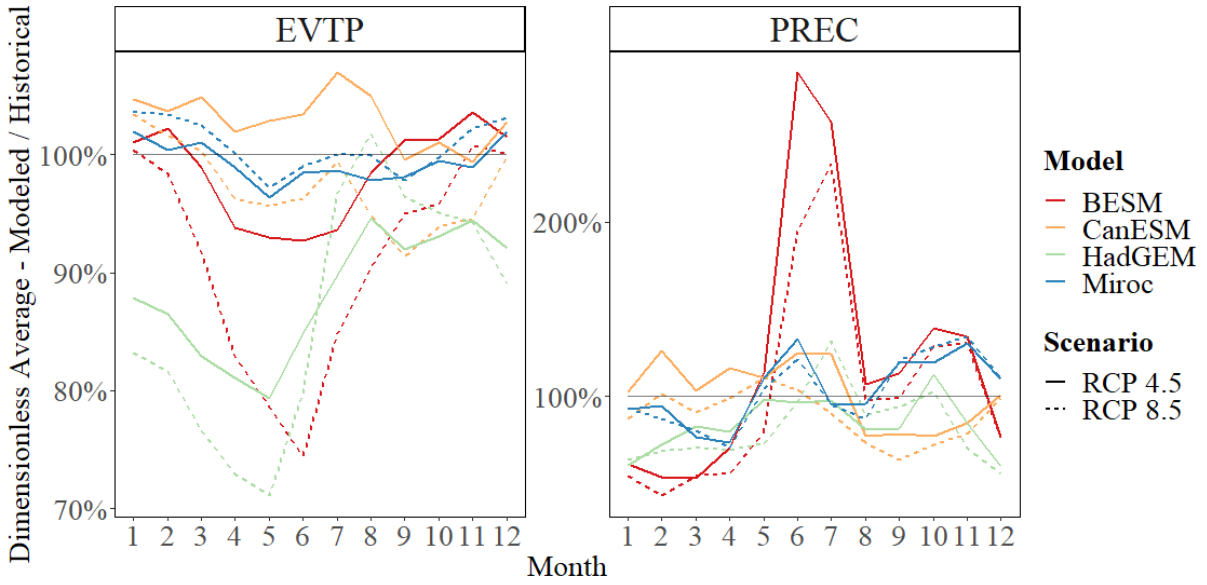

Source: Author (2023).

Figure 3 displays the precipitation data using the same climate models (Eta-BESM, Eta-CanESM, Eta-HadGEM, and Eta-Miroc) and RCP scenarios (RCP 4.5 and 8.5). This figure demonstrates a greater loss of water due to evapotranspiration and soil water evaporation. The data obtained from this first analysis can then be utilized in statistical models, such as SMAP, which will output a predicted river flow measurement.

To ensure accurate interpretation of nondimensional average analysis, it is crucial to consider the potential for misinterpretation. For instance, if we consider a dry period with a historical average rainfall of 10 mm and a model indicating an additional 10 mm of rainfall, the total rainfall would be 20 mm. Using non dimensional average analysis, this increase would be calculated as 100%, with the resulting line reaching 200%. This dramatic increase may visually impact the interpretation of the data. However, in a wet period with a rainfall of 200 mm, the same model showing a 10 mm increase would only result in a nondimensional average increase of 5%, and the resulting line would barely change. In both hypothetical scenarios, the increase in rainfall volume is the same, but the historical data differs. To avoid misinterpretation, special attention should be paid to the dry season from May through August.

The data presented can be further disaggregated by counties. To minimize the variability in climate models and identify trends in rainfall and its impacts for the next 100 years, the analysis was conducted on distinct scenarios and models. Figures 4 and 5 display the results of Eta-BESM RCP 4.5 and RCP 8.5 models, respectively. Figures 6 and 7 show the outcomes of Eta-CanESM RCP 4.5 and RCP 8.5 models. Similarly, Figures 8 and 9 illustrate the results of Eta-HadGEM RCP 4.5 and RCP 8.5 models, while Figures 10 and 11 display the findings of Eta-Miroc RCP 4.5 and RCP 8.5 models. In the figures, colors such as red and yellow indicate a reduction in rainfall, while blue and green represent an increase in rainfall.

Figure 4 - Variation in yearly rainfall under the Eta-BESM climate model and RCP 4.5 scenario

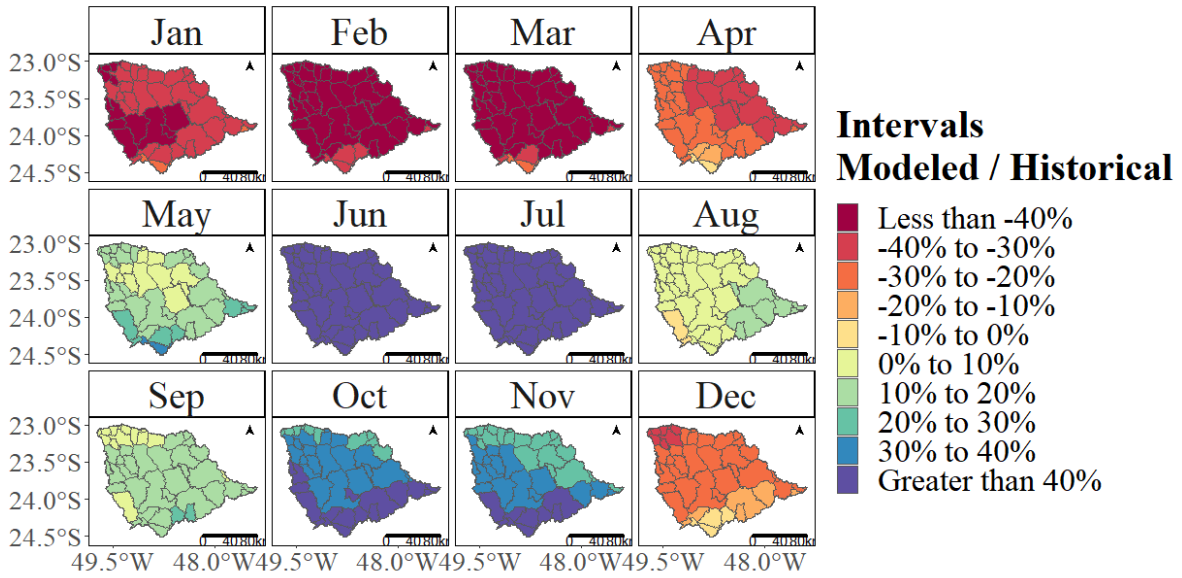

Source: Author (2023).

According to Figure 4, there is a visually noticeable increase in hydrological stress in the region. This is evident from the reduction in rainfall during the months of January to April. Additionally, the figure indicates an increase in rainfall during June and July, which are months of the dry season, and during October and November, which are months of the wet season. This pattern emphasizes the shift in rainfall regime due to climate change, as pointed by Chou *et al*. (2014).

Figure 5 - Variation in yearly rainfall under the Eta-BESM climate model and RCP 8.5 scenario

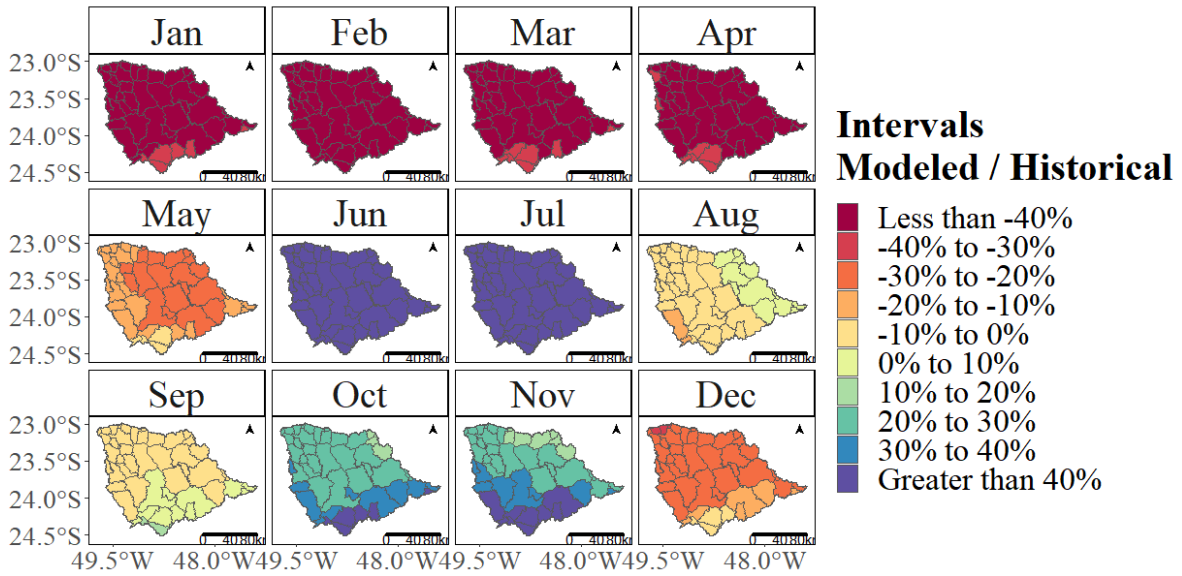

Source: Author (2023).

A comparison between Figures 4 and 5 illustrates the impact of climate change and the differences between RCP scenarios. Figure 5, which depicts the Eta-BESM climate model and RCP 8.5 scenario, visually demonstrates a more extreme scenario than that shown in Figure 4 (RCP 4.5 scenario). The reduction of rainfall during January through April is greater in Figure 5 than in the previous scenario, and the increase in rainfall during the wet season, mainly October and November, is smaller than in the RCP 4.5 scenario. These findings indicate that extreme events have a higher chance of occurring in the RCP 8.5 scenario. However, there is no significant change in rainfall during June and July.

Figure 6 - Variation in yearly rainfall under the Eta-CanESM climate model and RCP 4.5 scenario

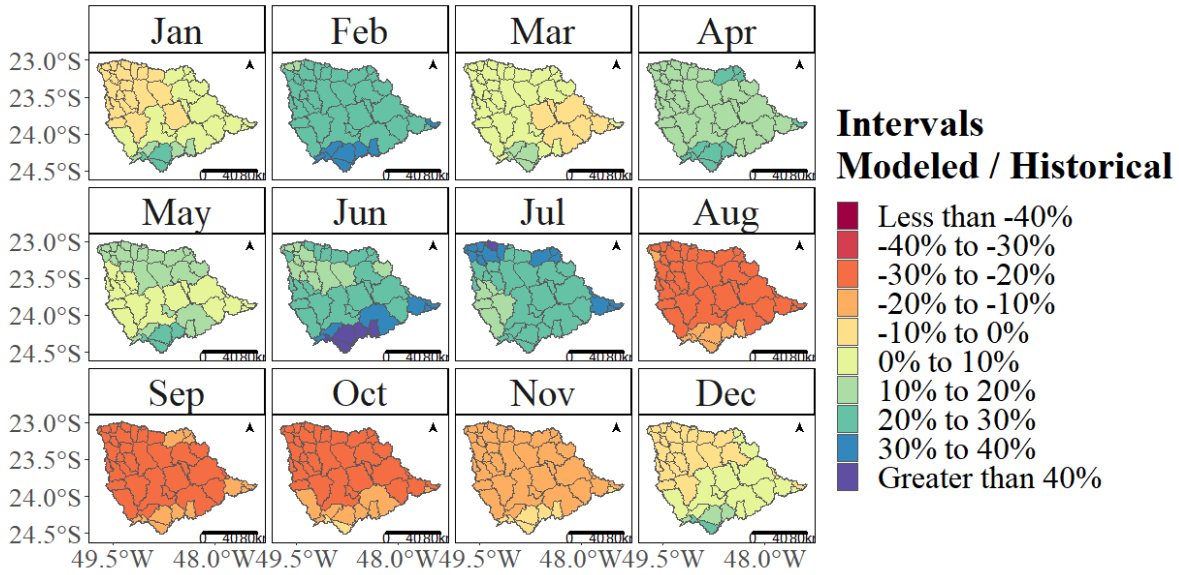

Source: Author (2023).

Figure 7 - Variation in yearly rainfall under the Eta-CanESM climate model and RCP 8.5 scenario

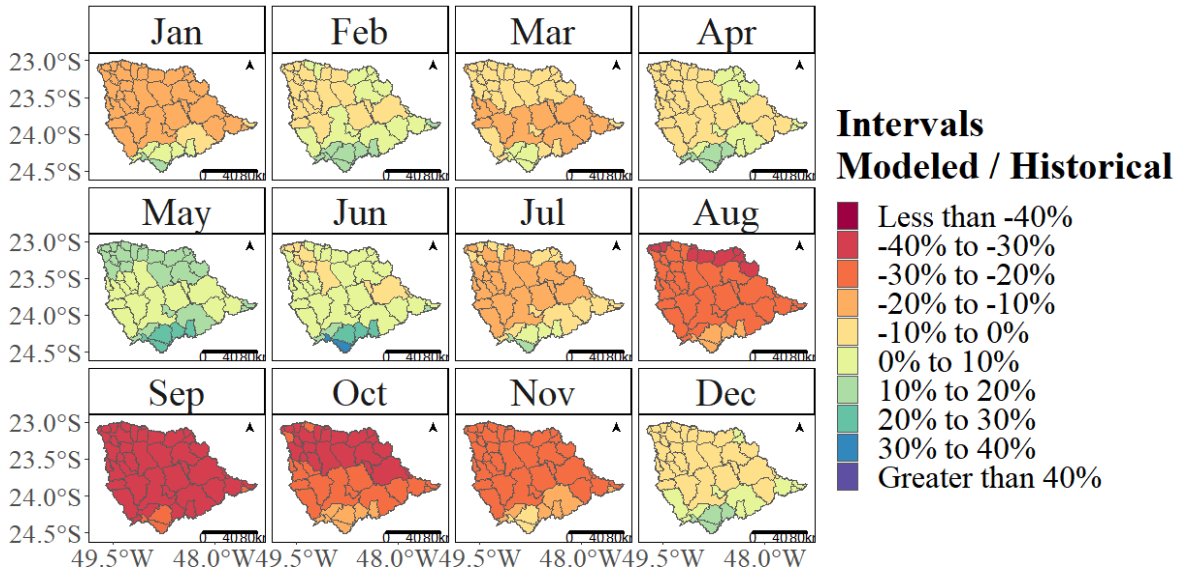

Source: Author (2023).

When comparing the Eta-BESM and Eta-CanESM models, a slight increase in rainfall during the dry season and a slight decrease in rainfall during the wet season can be observed.

Figure 8 - Yearly rainfall variation in the Eta-HadGEM climate model and RCP 4.5 scenario

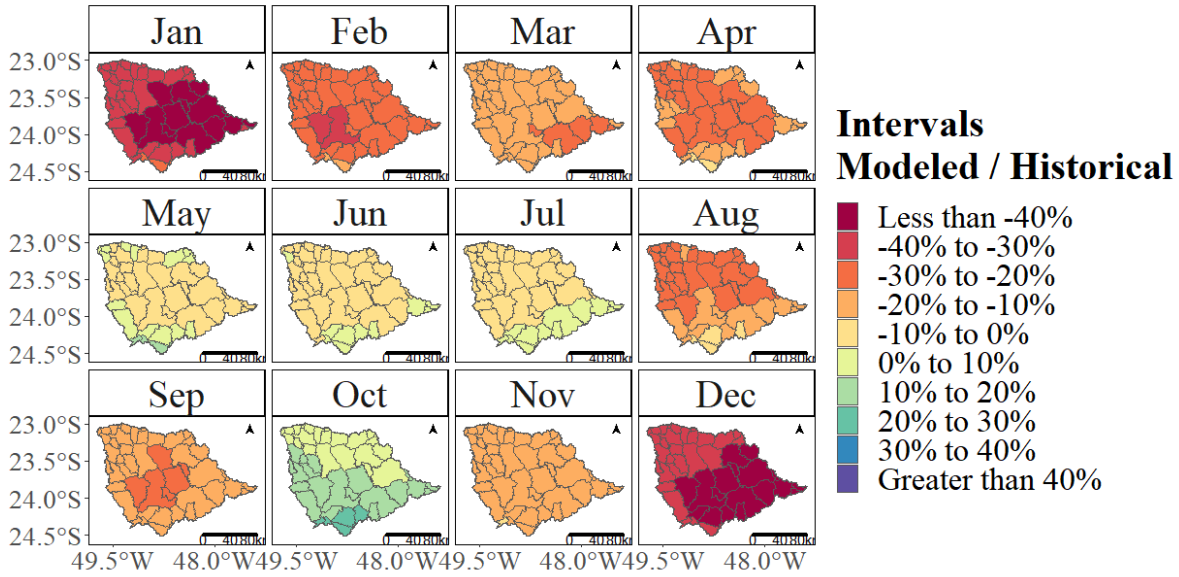

Source: Author (2023).

Figure 9 - Yearly rainfall variation in the Eta-HadGEM climate model and RCP 8.5 scenario

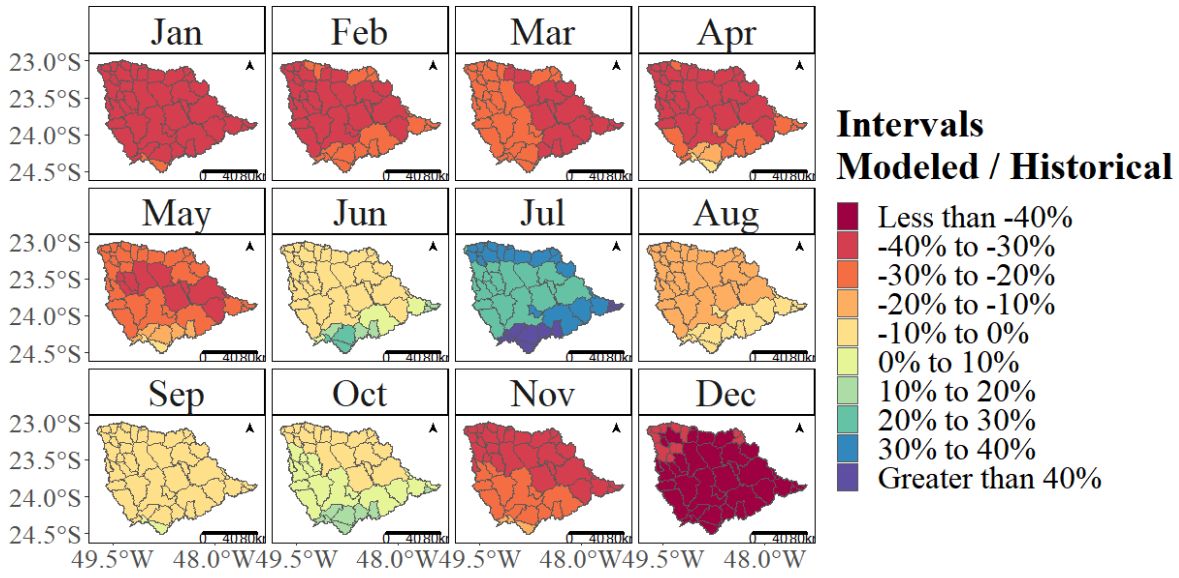

Source: Author (2023).

Comparison of the Eta-HadGEM model with the other models reveals that it combines the results of the previous two models. Specifically, during the dry season, the Eta-HadGEM model indicates less rainfall compared to the historical data, similar to the Eta-BESM model. Additionally, during the wet season, the Eta-HadGEM model shows a decrease in rainfall, although not as much as in the Eta-CanESM model.

Figure 10 - Yearly rainfall variation in the Eta-Miroc climate model and RCP 4.5 scenario

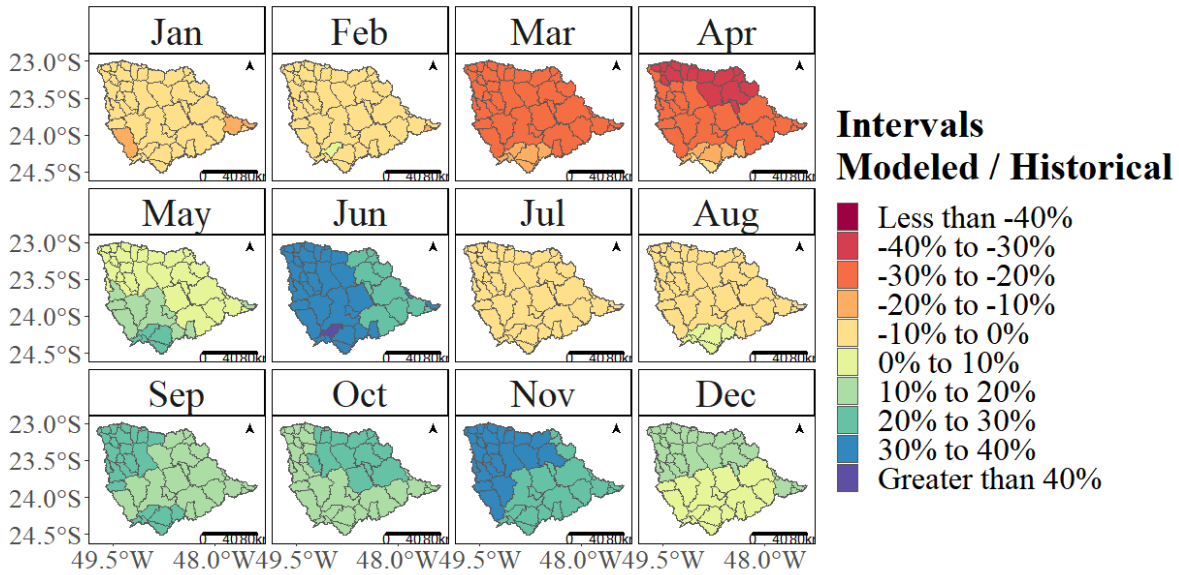

Source: Author (2023).

Figure 11 - Yearly rainfall variation in the Eta-Miroc climate model and RCP 8.5 scenario

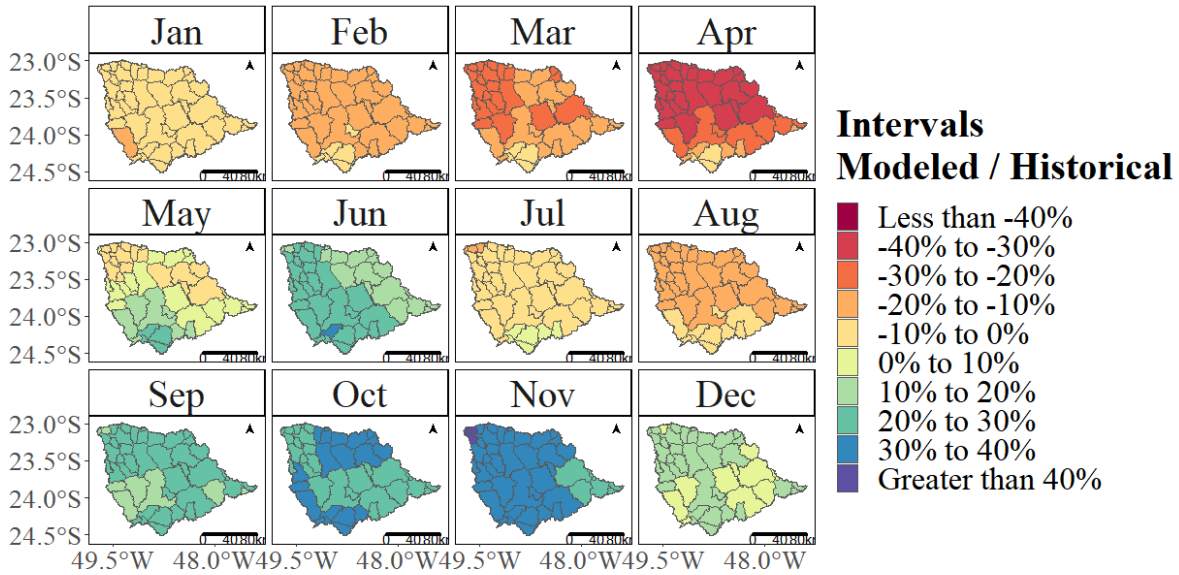

Source: Author (2023).

The Eta-Miroc model shares a similar trend to that of other models. However, the change in rainfall when compared to the historical data is more subtle than the other models, both in wet and dry seasons.

Three primary inferences regarding the trends in rainfall for the predicted years emerge. Firstly, there will be reductions in rainfall, with precipitation concentrated in fewer

months during the wet season. This will result in longer and more severe droughts, which will have a significant impact on sectors such as agriculture and power generation. Furthermore, the concentration of rainfall in fewer months may lead to extreme weather events occurring more frequently. Secondly, during the dry season, there will be an increase in rainfall, which could affect the agricultural sector by altering the optimal time to begin planting crops. This change could result in crop losses and have a negative impact on the economy. Finally, the third trend predicts an increase in rainfall during the wet season, accompanied by a reduction in rainfall during the dry season. This trend may lead to frequent storms that could damage pluvial water drainage systems in cities, cause soil erosion in rural areas, and create dangerous droughts for water supply and energy generation systems.

To gain a better understanding of the impacts on society, the analysis of rainfall should be converted to river flow. The comparison of historical data provides a valuable analysis, particularly with regards to the extreme hydrological events that occurred in the late 1970s and 1980s. When this data is converted into a line graph for the Jurumirim and Chavantes watersheds, as presented in Figure 12, the spike in river flow during this period is evident.

Figure 12 - Monthly river flow historical data and trend for the Chavantes and Jurumirim watershed

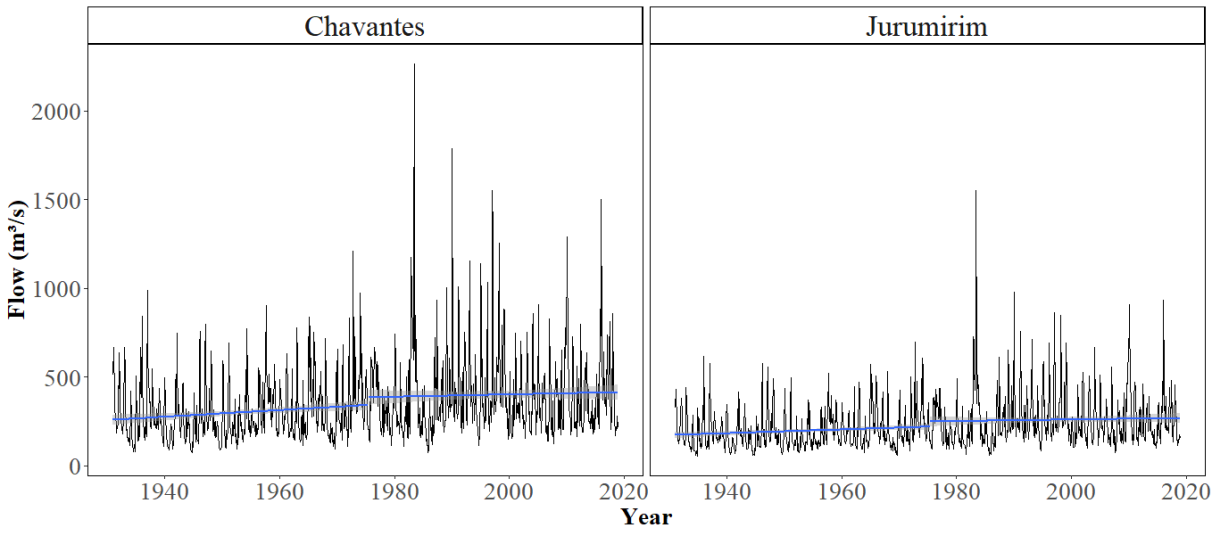

Source: Author (2023).

As indicated in the graphs, prior to the identified break, the river flow exhibited an annual increase, while after the break, the river flow stabilized. Had the break not been identified, the data would have suggested a steady increase in river flow over time. This new insight highlights the potential for both positive and negative changes in river flow, without

any abrupt changes in overall behavior. Figure 13 presents a comparison between the historical and predicted river flow.

Figure 13 - Compared average river flow for Chavantes and Jurumirim watersheds

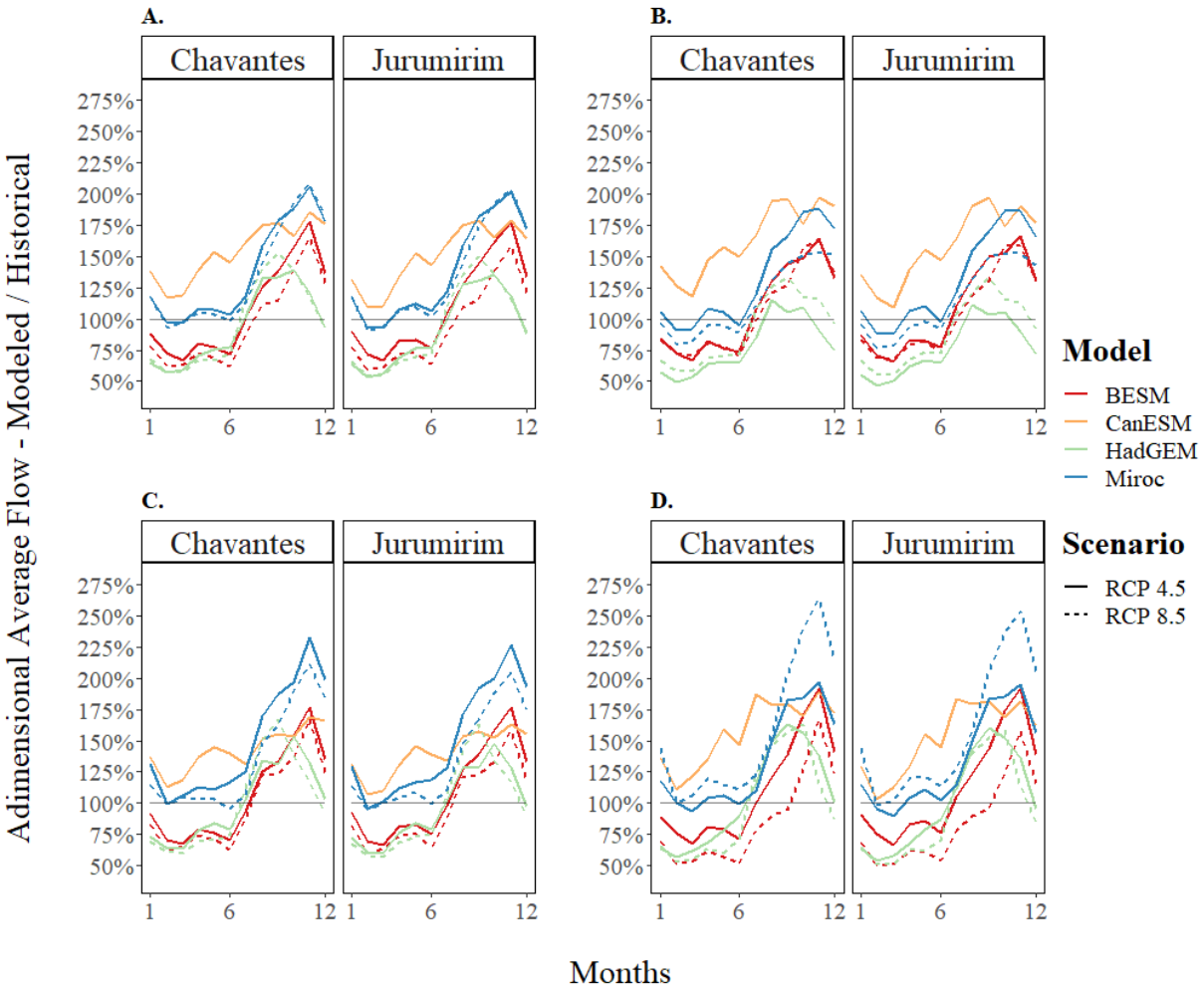

Source: Author (2023).

Legend: A) 2010 to 2099;

B) 2010 to 2039;

C) 2040 to 2069;

D) 2070 to 2099.

Located in the southwest of Brazil, the watersheds studied exhibit a known transient behavior that mimics a sine curve. This behavior is a result of their location in a transition zone between the atmospheric convergence zones of the north and south (Chou *et al*., 2014; Utida *et al*., 2019; Wong *et al*., 2021). During the wet season, there are losses from January to March and gains from October to December, with a steep drop in the latter month. In the dry season, losses occur from April to June and gains from July to September. Overall, losses account for approximately 60 % of the total, while gains can exceed 200 %. As with the

rainfall analysis, caution must be exercised in interpreting these values to avoid misinterpretation of the river flow data.

The RPC 8.5 scenario presents a less optimistic outlook, with greater losses and less accentuated gains when compared to RPC 4.5. The Eta-Miroc model, on the other hand, shows an interesting trend in the two different scenarios, with a smaller difference between them than other models. This trend can be better visualized when the data is broken down by climate normals, as shown in Figure 13 B, C and D.

The Eta-Miroc model demonstrates that under the last climate normal, the RPC 8.5 exhibits a greater decrease in river flow compared to RPC 4.5, highlighting the notion that climate change is not solely correlated with a reduction in rainfall and river flow, but also with changes in atmospheric behavior that affect the amount, timing, and location of rainfall. While the data is divided into climate normals, they still display a sine curve pattern like that of Figure 13. Furthermore, these graphs reveal a potential decrease in river flow over the next century, with the largest decrease occurring in the latter half of the graph. To further illustrate this decline in river flow, single graphs with trend lines have been presented in Figure 14.

Figure 14 - Predict river flow and trend line year by year from 2010 to 2099 for Chavantes and Jurumirim watersheds

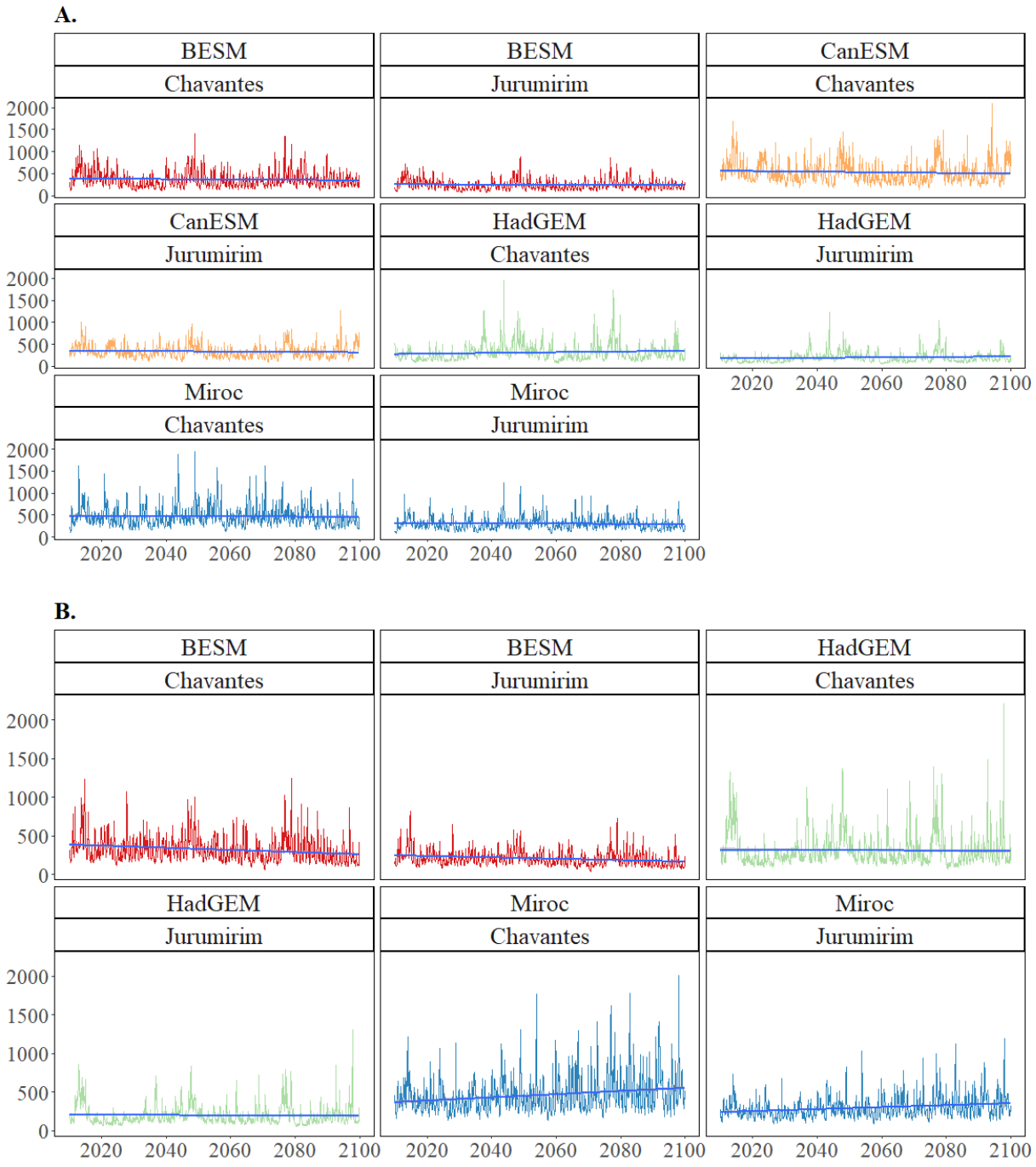

Source: Author (2023).

Legend: A) RCP 4.5;

B) RPC 8.5.

All trend lines point to river flow reduction, with two exceptions. First, the model Eta-HadGEM RPC 4.5, presents a slight increase in river flow. This fact can be attributed to a contradiction in the model for the study area, that tends to have a bigger rainfall response than

other models. The second exception is Eta-Miroc in RCP 8.5 scenario that emphasizes the climate normal discussion.

4 CONCLUSION

Water management is a crucial issue in the Alto Paranapanema Basin, given its importance as a source of water supply for different sectors of society. Effective water management requires collaboration and communication between basin management units to ensure sustainable use of water resources. In addition, it is essential to develop and use predictive models to anticipate potential changes in water availability and demand.

For instance, the Chavantes and Jurumirim watersheds may experience a reduction in flow in the coming years due to various factors, including increasing population and water consumption, changing land use, and soil impermeability, as seen with the increase in agriculture pivots use. By themselves, these factors can alter the basin's hydrological cycle and lead to water scarcity, as seen in some Brazilian locations. When combining this threat with impacts of climate change, the water scarcity deepens, not only impacting the studied headwater sub basin, but all other downstream basins.

Furthermore, climate change can also lead to the displacement of rains to other regions of the country, affecting agricultural production and other land uses in the Alto Paranapanema Basin. This can pose significant challenges for farmers and land managers, who must adapt to changing weather patterns and water availability. To address these challenges, it is necessary to encourage studies of rainfall predictions and climate change scenarios that can help water managers make informed decisions about water allocation and use.

Climate modeling data are critical for water managers to mitigate and minimize the adverse effects of climate change on society. By using predictive models and sharing information between basin management units, we can better manage water resources and ensure their sustainable use for future generations.

REFERENCES

INTERNATIONAL PANEL FOR CLIMATE CHANGE. Technical summary. **Cambridge University Press**, Cambridge, United Kingdom and New York, NY, USA, pp. 33-144, 2021.

AGÊNCIAS NACIONAL DE ÁGUAS. Levantamento da agricultura irrigada por pivôs centrais no Brasil. Agência Nacional de Águas, **Embrapa Milho e Sorgo. - 2. Ed.**, Brasília, Brasil, 2019.

BARROS, M. T. L., *et al*. Climate flow forecast model for the Brazilian hydropower system. **World Environmental and Water Resources Congress 2009: Great Rivers**, [*s. l.*], 2019.

BARROS, G.S.C., *et al.* Boletim PIB do agronegócio, São Paulo -2020. **Centro de Estudos Avançados em Economia Aplicada**, [*s. l.*], 2021.

CHOU, S. C., *et al*. Assessment of climate change over South America under RCP 4.5 and 8.5 downscaling scenarios. **American Journal of Climate Change**, [*s. l.*] 03(05), 512–527, 2014.

CHOU, S. C., *et al*. Evaluation of the ETA simulations nested in three global climate models. **American Journal of Climate Change**, [*s. l.*], 03(05), 438–454, 2014.

COMMONER, B. The closing circle: nature, man, and technology. **Courier Dover Publications**, [*s. l.*], 2020.

EMBRAPA. Georreferenciamento dos pivôs centrais de irrigação no Brasil: ano base 2020. **Sete Lagoas: Embrapa Milho e Sorgo**, 2020. Available at: https://www.infoteca.cnptia.embrapa.br/infoteca/handle/doc/1128368. Accessed in: July of 2023.

GREEN, T. R., *et al*. Beneath the surface of global change: Impacts of climate change on groundwater. **Journal of Hydrology**, [*s. l.*], 405(3), 532–560, 2011.

GUEYMARD, C. A. Clear-sky irradiance predictions for solar resource mapping and large-scale applications: improved validation methodology and detailed performance analysis of 18 broadband radiative models. **Solar Energy**, [*s. l.*], 86(8), 2145–2169, 2012.

BRAZILIAN INSTITUTE OF GEOGRAPHY AND STATISTICS. **Brazilian official data of economics resources**, 2023. Available at: https://ibge.gov.br/explica/pib.php/. Accessed in: July of 2023.

JACKSON, R. B., *et al*. Water in a changing world. **Ecological Applications: A Publication of the Ecological Society of America**, [*s. l.*], 11(4), 1027–1045, 2001.

LOPES, J. E. G., BRAGA, B. P. F. & CONEJO, J. G. L. SMAP - A simplified hydrological model. In: Applied modeling in catchment hydrology, V.P. Singh (ed.), **Water Resources Publications**, Littleton, CO, USA, 167-176, 1982.

LYRA, A., *et al*. Climate change projections over three metropolitan regions in Southeast Brazil using the non-hydrostatic Eta regional climate model at 5-km resolution. **Theoretical and Applied Climatology**, [*s. l.*], 132(1), 663–682, 2018.

MARAUN, D., *et al*. Precipitation downscaling under climate change: Recent developments to bridge the gap between dynamical models and the end user. **Reviews of Geophysics**, 48(3), [*s. l.*], 2010.

NASH, & SUTCLIFFE. River flow forecasting through conceptual models part I—A discussion of principles**. Journal of Hydrology**. [*S. l.*], 1970.

O'NEILL, P., *et al*. Soil Moisture Active Passive (SMAP) mission: Overview. **2010 IEEE International Geoscience and Remote Sensing Symposium**, [*s. l.*], 3236–3239, 2010.

PENG, J., *et al*. A roadmap for high-resolution satellite soil moisture

applications–confronting product characteristics with user requirements. **Remote Sensing of the Environment**. [*S. l.*], 2021.

SKAGGS, R. W., BREVÉ, M. A., & GILLIAM, J. W. Hydrologic and water quality impacts of agricultural drainage. **Critical Reviews in Environmental Science and Technology**, 24(1), 1–32, [*s. l.*], 1994.

TIEZZI, R. O., *et. al.* Impacts of climate change on hydroelectric power generation – A case study focused in the Paranapanema Basin, Brazil. **Journal of Sustainable Development in Africa**, 11(1), 140, [*s. l.*], 2018.

TIEZZI, R. O., *et al*. Trends of streamflow under climate change for 26 Brazilian basins. **Water Policy**, 21(1):206–220, [*s. l.*], 2019.

UTIDA, G., *et al*. Tropical South Atlantic influence on Northeastern Brazil precipitation and ITCZ displacement during the past 2300 years. **Scientific Reports**, 9(1), 1–8, [*s. l.*], 2019.

VAN VUUREN, D. P., *et al.* The representative concentration pathways: an overview. **Climatic Change**, 109(1), 5, [*s. l.*], 2011.

WIGNERON, J.-P., *et al.* Modeling the passive microwave signature from land surfaces: A review of recent results and application to the L-band SMOS & SMAP soil moisture retrieval algorithms. **Remote Sensing of Environment**, 192, 238–262, [*s. l.*], 2017.

WONG, M. L., *et al*. Variations in the South Atlantic Convergence Zone over the mid-to-late Holocene inferred from speleothem δ18O in central Brazil. **Quaternary Science Reviews**, 270, 107178, [*s. l.*], 2021.

ZHANG, D., & ZHOU, G. Estimation of soil moisture from optical and thermal remote sensing: A review. **Sensors**, 16(8), [*s. l.*], 2016.

ZHANG, X., *et al*. Impacts of climate change, policy and Water-Energy-Food nexus on hydropower development. **Renewable Energy**, 116, 827–834, [*s. l.*], 2018.

2.7 Artigo II: A comparative analysis of widespread used hydrological tools and neural networks models

Andre T. S Hucke[1]
Mateus Menegaz[2]
Jorge Isidoro[3]
Rafael de Oliveira Tiezzi[4 *]

Abstract

Streamflow prediction is critical for Brazil, where over 70% of power generation depends on dams. Traditional hydrological models, such as Soil Moisture Accounting Procedure (SMAP) and Linear Stochastic Model (LSM), coexist without clear superiority. In recent years, machine learning, including Artificial Neural Networks (ANN), Support Vector Machines (SVM), and Long Short-Term Memory (LSTM), has gained prominence. Convolutional Neural Networks (CNN) excel in image recognition, and Recurrent Neural Networks (RNN) show promise in forecasting. Most RNN studies focus on short-term predictions, neglecting climate inputs. Calibrating and validating models remain active research topics, while Global Climate Models (GCMs) and regionalization play pivotal roles in understanding climate change impacts. A comparative study of neural networks and mainstream tools for streamflow prediction in 25 Brazilian basins using precipitation and evapotranspiration inputs provides insights into future water management amid varying climate conditions and demands.

Keywords: *Streamflow Prediction, Hydrological Models, Neural Networks, Climate Change Impacts, Brazil Water Management*

---

[2] [1, 2] Institute of Science and Technology, Federal University of Alfenas, Rodovia José Aurélio Vilela, 11999 (BR 267 Km 533), Cidade Universitária, Poços de Caldas, MG CEP 37715-400, Brazil. andre.hucke@sou-unifal.mg.edu.br. matmenegaz@hotmail.com.
[3] University of Algarve. jorge.mgp.isidoro@gmail.com
[4] Institute of Science and Technology, Federal University of Alfenas, Rodovia José Aurélio Vilela, 11999 (BR 267 Km 533), Cidade Universitária, Poços de Caldas, MG CEP 37715-400, Brazil. rafaeltiezzi@ufscar.br
* Corresponding Author: rafaeltiezzi@ufscar.br

1 INTRODUCTION

Streamflow is an important metric for policy makers as more than 70% of Brazil's power generation is dams. Other than power generation, we also have noble uses such as human consumption, livestock watering and irrigation. A good future hydrological prediction becomes essential to evaluate long term water usage avoiding droughts of existing dams and find the best locations to implement new dams (de Oliviera Junior *et al*., 2018). Hydrologists have developed two main methods, namely Soil Moisture Accounting Procedure (SMAP) and Linear Stochastic Model (LSM), for predicting streamflow (Duan, Sorooshian and Gupta , 1992). While these models are widely used, there is no objectively superior model, and often both models are used complementary (Xu, 1999).

Recently, machine learning and artificial intelligence have gained popularity in various fields, from video games to personalized medicine. These approaches enable exploration of relationships within data that traditional analysis may struggle to identify. In the field of hydrology, data-driven neural networks such as Artificial Neural Networks (ANN), Support Vector Machines (SVM), and Long Short-Term Memory (LSTM) have been employed in complex hydrological studies (Marr, 2019). Furthermore, some studies use decomposition methods to establish the physical relationships between streamflow and climate (Cui *et al*., 2018).

Artificial neural networks (ANN) have two main architectures: convolutional neural networks (CNN) and recurrent neural networks (RNN) (LeCun, Bengio and Hinton, 2015; Lipton, Berkowitz and Elkan, 2015). ANN can be supervised or unsupervised (Bishop, 2006), online or batch (Duchi, Hazan and Stinger, 2011), instance-based or model-based learning (Mitchell, 1997). Supervised learning means that the model has labels for its dataset and learns the relationship between the features and the labels (Bishop, 2006). Unsupervised learning only has the feature and tries to find similarities in those features to cluster them together (Bishop, 2006). Online learning means that the model learns from a constant stream of information, while batch learning the model learns from all available data at any given moment and has to be retrained if new data is added (Duchi, Hazan and Stinger, 2011). Instance-based learning is when a model uses what it learns from the data to predict what a new instance is by using similarity with the learned data (Mitchell, 1997). Model-based learning generalizes the input data to make predictions (Mitchell, 1997).

The CNN is a feedforward NN that is widely applied to image recognition (LeCun, Bengio and Hinton, 2015). It takes in features to extract relationships out of them or predict

possible labels (LeCun, Bengio and Hinton, 2015). An example of image application would be tumorous cancer size and detection (Munir *et al*., 2016). There is also use for forecasting financial time series, which can be similar to hydrology for a machine (Fischer and Krauss, 2018).

The RNN has been extensively used for various applications, including forecasting and natural language processing, due to its ability to use the output of a neuron as the input of the next neuron (LeCun, Bengio and Hinton, 2015; Vaswani *et al*., 2017). However, in the field of hydrology and fluid mechanics, the use of RNNs is still in its early stages and requires further development and research to become an addition to mainstream models (Kratzert *et al*., 2018). Most studies in the area do not use climate as an input for ANN and use a LSTM approach to predict the streamflow (Jia Wang *et al*., 2020; Jia Wang, Wang and Khu, 2023; Thao-Tsen Chen and Lee., 2015; Sahoo *et al*., 2019; Sahoo *et al*., 2019).

There are various models used for short-term predictions in hydrology and fluid mechanics, including SMAP, which is a deterministic model that uses physical parameters, and LSM, which is a statistical model that can generate flows below zero and may suffer from gradient explosion (Medina *et al*. 2021). However, when it comes to long-term predictions, minor alterations in input variables can significantly impact the results (Kratzert *et al*., 2018).

Calibrating a model means that we estimate a model's parameters and compare the model's output from a known period and conditions with observations from the same period and conditions. Validating a model is to take the calibrated parameters and use them to run the model for a new input data for the same calibrated basin. Measurement and assessment of these models are still widely discussed in the scientific field and acquiring deeper knowledge of this field is critical. Calibrating and validating models are crucial steps in the development of hydrological models, and measuring and assessing their performance is still an ongoing topic of research (Oliva, 2003).

Global Climate Models (GCMs) are complex mathematical climate models that aim to simulate the Earth's climate system, and they are used to predict future climate scenarios under different greenhouse gas emission scenarios (Collins *et al*., 2013). These climate models are developed and provided by several institutions, including the Canadian Centre for Climate Modelling and Analysis, the Center for Climate System Research, the National Institute of Space Research (INPE), and the Met Office Hadley Centre. The predictions provided by GCMs are used as input to stochastic climate models, which generate climate projections called Representative Concentration Pathways (RCPs) (van Vuuren *et al*., 2011).

To enhance the accuracy of GCMs, researchers often perform a process called downscaling or regionalization. This involves incorporating additional variables, such as topography, land use, or local climate data, that are specific to the region under analysis. In Brazil, the regionalization process is performed by INPE, which uses multiple GCMs to generate more accurate and reliable predictions of future climate scenarios in Brazil (Chou *et al*., 2014).

Overall, GCMs and their regionalized versions play a critical role in helping policymakers and researchers understand the potential impacts of climate change at different scales, from global to regional. They provide valuable insights into the complex and interconnected processes that govern our climate system and help us make informed decisions to mitigate and adapt to climate change.

With that in mind, we compared 25 most impactful basins in Brazil aiming to compare neural networks approaches with the mainstream tools, using precipitation and evapotranspiration as inputs and streamflow as labels aiming to obtain predicted streamflows for a dataset provided by National Institute of Space Research (CPTEC/INPE). Having yet another method of predicting the future could bring more insight to future water flow in rivers, whether it is an increase or decrease in flow. This water is turned into volumes in reservoirs and dams. This volume is then used in power generation, human consumption, watering animals, tourism and many other uses that can have conflicts of priorities when faced with droughts.

2 METHODS

For this study, we collected information of precipitation, evapotranspiration and streamflow at discharge for the 25 top producing basins in Brazil. They are represented in Figure 1. Although Tapajós is shown, it was excluded from this study as the data was not comparable to the other basins.

Figure 1- Basins for the present study

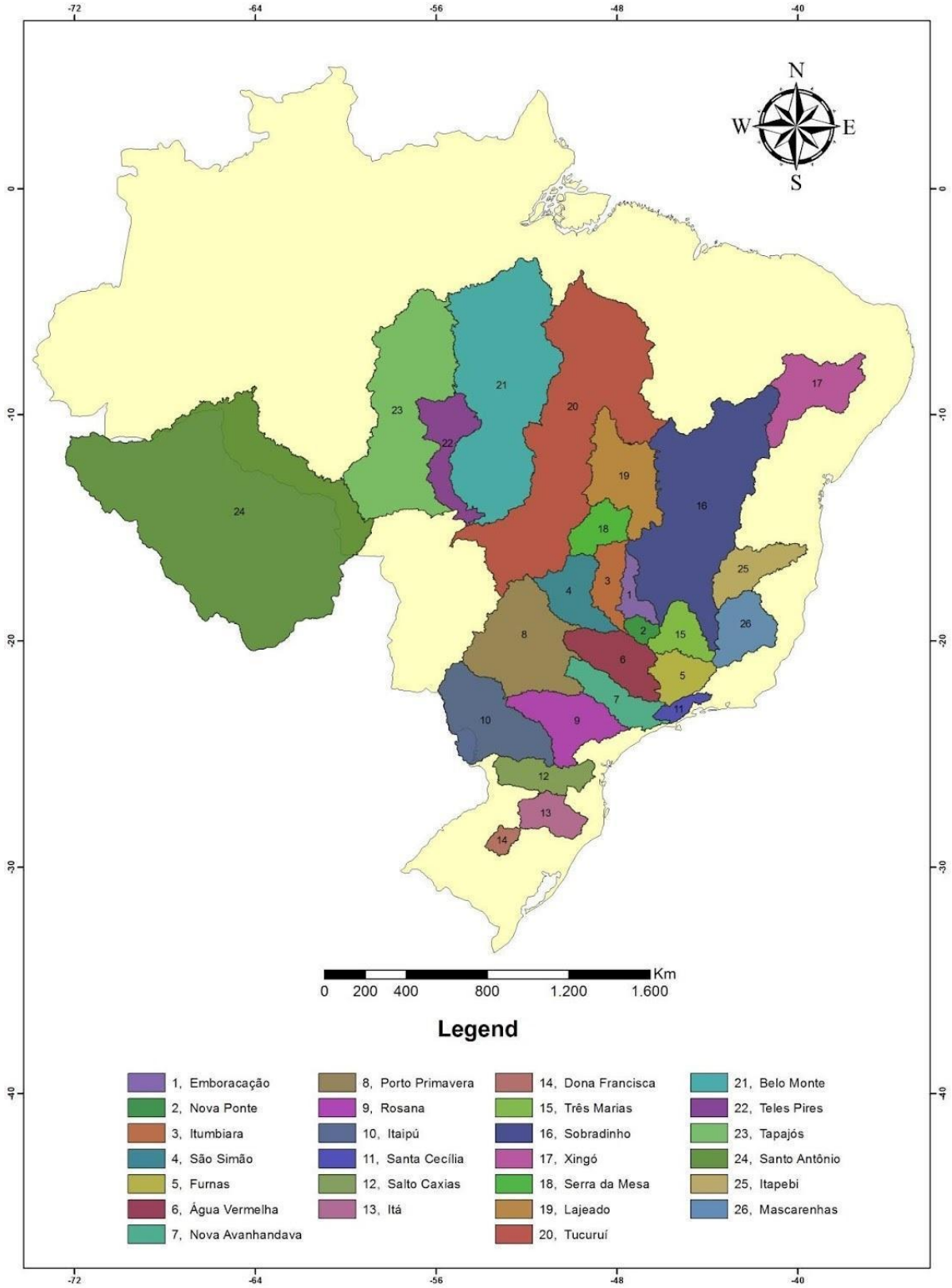

Source: Adapted from Tiezzi, 2014.

The data provided by INEP is a dataset that was preprocessed in ArcGIS to obtain precipitation and evapotranspiration means for the basin and it ranges from 2010 to 2100. A known fact in Brazil hydrological data is the lack of and sometimes bad quality of the available data. This can affect the training step of neural networks, as they analyze the patterns of this data and if they are given bad data, they will produce bad results. That proved to be an issue where the already very limited data for the ANN input could not break down even further. So, for validation we chose 5 (five) basins that also had good quality data for the years of 2002 to 2011. The present study used a previous study for calibrations and validations for SMAP and LSM (Tiezzi, 2014).

To simulate and optimize the representation of climate patterns in global climate models (GCMs), various institutions model these systems using diverse grid sizes that typically range from 400 × 400 km to 200 × 200 km. Subsequently, regional climate models (RCMs), such as the Eta climate model, use the information from GCMs to focus computational efforts on enhancing the prediction of precipitation in specific regions of the world (Chou *et al*., 2014).

In the present study, GCMs were utilized, and their characteristics and features were summarized in Table 1 (Chou *et al*., 2014; Lyra *et al*., 2018). These climate models are crucial for predicting future climate conditions and making informed decisions regarding climate change mitigation and adaptation strategies.

Several studies have evaluated the performance of GCMs and their ability to simulate past and future climate scenarios accurately (Flato *et al*., 2013; Collins *et al*., 2021). Further, advancements in computing technology and the availability of more extensive datasets have allowed for the development of high-resolution climate models with improved accuracy (Flato *et al*., 2013).

Modeling and simulation of GCMs, followed by the use of RCMs, can help improve our understanding of climate patterns and provide insights into potential future scenarios. These advancements can inform policy decisions and aid in developing strategies for mitigating and adapting to climate change.

Table 1 - GCMs models and its characteristics. Source: Author.

Climate model	Institution	Resolution (lat^{o} x long^{o})	Levels	Vegetation	Addition information

BESM	National Institute for Space Research, Brazil	0.25º to 2º × 1º	28 terrestrial and 50 oceanic	12 different types	Radioactive interactions and convective cloud system
CanESM2	Canadian Center for Climate Modeling and Analysis, Canada	2.8125º × 2.8125º	35 atmospheric	9 different types in 3 different vegetative systems	Carbon cycle components and dead organic matter
HadGEM2-EM	Met Office Hadley Center, United Kingdom	1.875º × 1.25º	38 atmospheric	5 different types	Climate model with atmospheric chemistry with aerosols
Miroc5	Japan Agency for Marine-Earth Science and Technology, Atmosphere and Ocean Research Institute, Japan	1.41º × 1.41º	40 terrestrial and 50 oceanic	3 groups	Uses albedo of snow and water mirrors. Also uses clouds microphysics

The Eta climate model is a numerical weather prediction climate model that has been adapted for downscaling global climate models (GCMs) to regional scales, particularly in Central and South America. Since its inception in 1997, the Eta climate model has been used by the Center for Weather Forecasting and Climate Studies (CPTEC/INPE) for short-term meteorological forecasting. In recent years, the Eta climate model has also been employed to investigate climate change scenarios based on GCM projections.

The Eta climate model incorporates various physical processes, including the annual dynamics of the microphysical vegetation cycle of clouds, a convective cloud scheme, and short- and long-wave radiation balance under constant CO2 concentration. It has a vertical resolution of 38 levels and a spatial resolution of 20 km, which allows for more detailed regional modeling (Chou *et al*., 2014).

In order to study the impacts of climate change on streamflow, the Eta climate model was coupled with four GCMs, namely Eta-BESM, Eta-CanESM, Eta-HadGEM2-ES, and Eta-Miroc5. Monthly precipitation and evapotranspiration data were obtained from these

climate models for the period between 1960 and 1989, as well as for the future period from 2010 to 2100 based on Representative Concentration Pathways (RCPs).

It is worth noting that while the Eta climate models generate a significant amount of data, only precipitation and evapotranspiration were used in this study to model the rainfall into the streamflow process. This is because precipitation and evapotranspiration are the primary drivers of streamflow, and therefore, they provide a good basis for studying the impact of climate change on streamflow (Chou *et al*., 2014).

Overall, the Eta climate model has proven to be a valuable tool for downscaling GCMs and studying the impacts of climate change on regional scales, particularly in Central and South America. Its high resolution and incorporation of various physical processes make it a powerful tool for investigating the complex interactions between climate and the environment.

For the RCPs scenarios, the present study used the RCP 4.5, the least extreme greenhouse concentration scenario and RCP 8.5, the most extreme scenario. The CanESM RCP 8.5 scenario was excluded, as it was not possible to gather information about this specific scenario from CPTEC/INPE.

Uniform Manifold Approximation and Projection (UMAP) is a widely used nonlinear dimensionality reduction technique that preserves both local and global structures of high-dimensional data (McInnes *et al*., 2018). UMAP has been shown to outperform t-SNE in terms of scalability and preserving global distances (Becht *et al*., 2019). In this context, UMAP is a suitable tool to visualize the overlap between different models, which indicates their similarity and consistency in predictions.

Optimizer is NADAM with a loss function that relies on mean squared error for all ANN. For calibration, we chose 60 data points of precipitation and evapotranspiration of selected, high quality data from January 1997 to December 2001. Both CNN and RNN were trained in a single batch for 4000 epochs with a learning rate of 0.01, based on trial and error. To mitigate possible overfitting and exploding gradients, we used a callback function that evaluates the previous 500 steps and stops the training earlier if it identifies that the loss did not improve over these steps.

To run the ANN’s, we chose a supervised learning method with the labels as the streamflow for a known period. The CNN doesn't have the same look back functionally as the RNN. To combat this and align the CNN with the mainstream tools, we used the output of a first CNN run as a new flow input of a new CNN with the same architecture, and it was called second CNN run. It is the only way of getting streamflow values for the future precipitation

without using another tool. They were copied and shifted the table to have the precipitation of the last 3 days as new inputs, artificially increasing the amount of features. The ANN targets are the streamflow for a known period with two main features: precipitation and evapotranspiration. These features and labels were normalized with a simple minimum maximum scaler, ranging from 0 to 1. Additionally, it was also proposed to use the output of the SMAP model as one of the inputs for the ANN run, following the same logic as previously stated for the second CNN run, called CNN-SMAP run. This described workflow is shown in the Figure 2 below.

Figure 2 - Workflow demonstrating inputs and outputs for each model analyzed

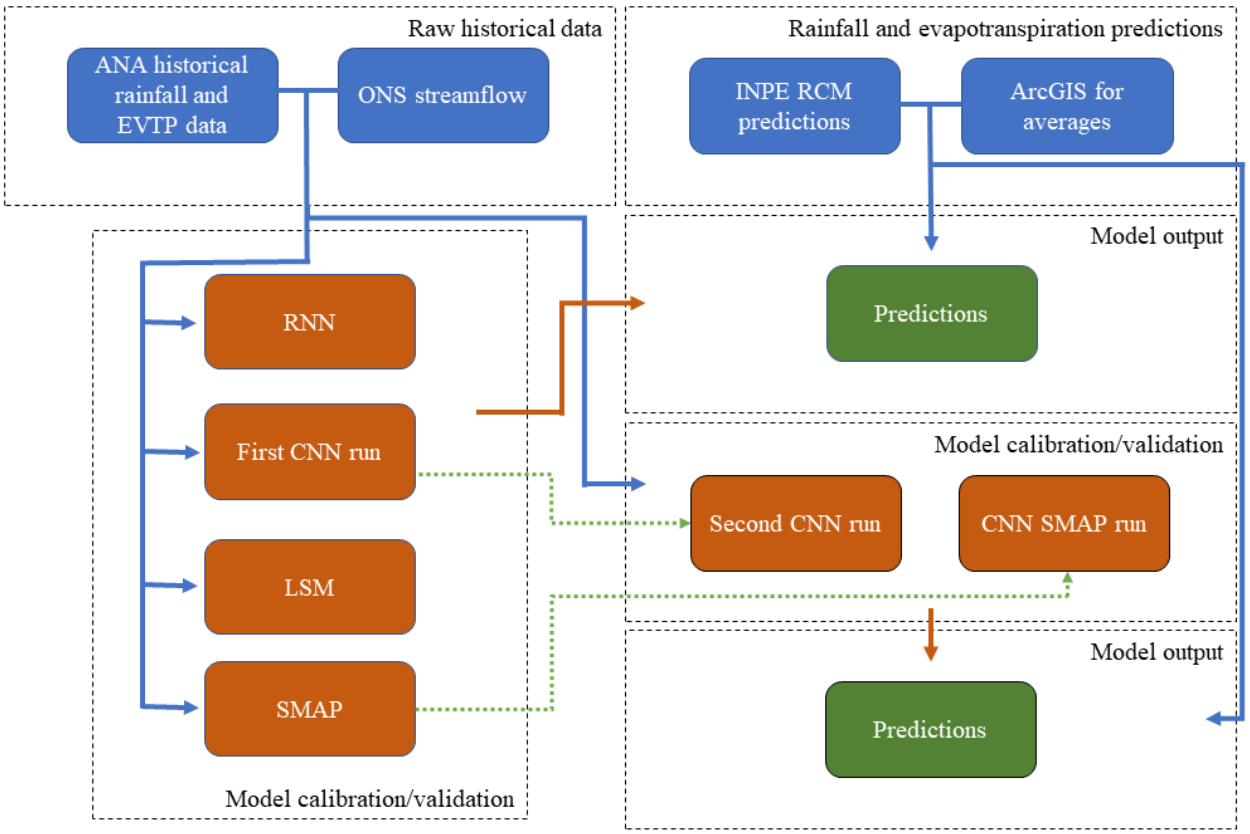

Source: Author (2023).

The layers and architecture used in the ANN are provided in Table 1 and Table 2.

Table 1- Layers for CNN architecture. Source: Tensorflow.

Layer (type)	Output Shape	Param #
dense (Dense)	(None, 15)	45
dropout (Dropout)	(None, 15)	0

dense_1 (Dense)	(None, 15)	240
dropout_1 (Dropout)	(None, 15)	0
dense_2 (Dense)	(None, 15)	240
dropout_2 (Dropout)	(None, 15)	0
dense_3 (Dense)	(None, 1)	16

Table 2 - Layers for RNN architecture. Source: Tensorflow.

Layer (type)	Output Shape	Param #
conv1d_1 (Conv1D)	(None, 60, 32)	96
max_pooling1d_1 (MaxPooling 1D)	(None, 60, 32)	0
lstm_1 (LSTM)	(None, 60, 15)	2880
dropout_1 (Dropout)	(None, 60, 15)	0
lstm_2 (LSTM)	(None, 60, 15)	1860
dropout_2 (Dropout)	(None, 60, 15)	0
dense_1 (Dense)	(None, 60, 1)	16

A good rule of thumb was used to choose the amount of neurons hidden layers (Neural Networks Design):

$$N_h = \frac{N_s}{(\alpha * (N_i + N_o))} \quad (1)$$

Where:

N_h is the number of neurons.

N_s is the number of samples in the training data set.

N_i is the number of inputs.

N_o is the number of output neurons.

α is an arbitrary number between 2 and 10, normally favoring lower numbers to avoid overfitting.

A sigmoid activation function was chosen to keep the output streamflow above zero, since there is no negative flow, and then it was descaled using the same minimum maximum scaler.

SMAP model uses Excel's SOLVER to optimize Nash-Sutcliffe coefficient (Nash & Sutcliffe, 1970). This model calculates flow based on precipitation and evaporation and is considered to be a type of concentrated parametric model. Based on the amount of data available, the model only runs off of precipitation and evapotranspiration data. The user also needs to input the basin size, soil permeability, base flow and soil moisture content, ideally after a dry period.

The LSM model is a transference function with multiple inputs. This model correlates current average precipitation, past precipitation and past gradient flow to obtain current gradient flow. Surface runoff is accounted for by dividing the precipitation in different isochrones.

Nash-Sutcliffe model efficiency coefficient (NSE) is a normalized statistical index that determines the relative magnitude of the residual variance when compared to the variance of the observed series and has an optimal value of 1. Negative values of NSE indicate that the mean values of the observed series is a better predictor. It follows the formula shown below:

$$NSE = 1 - \left[\frac{\Sigma_{i=1}^{n}\left(Y_i^{obs} - Y_i^{sim}\right)^2}{\Sigma_{i=1}^{n}\left(Y_i^{obs} - Y^{mean}\right)^2}\right] \quad (2)$$

Where:

Y^{mean} is the mean of observed streamflow.

Y_i^{sim} is the modeled streamflow.

Y_i^{obs} is the observed streamflow at time t.

Percent bias (PBIAS) optimal value is 0 and measures the tendency of the predicted value to be greater or lower than the observed series. Positive values indicate model underestimated while negative values indicate overestimation bias. PBIAS and NSE are often paired together to analyze hydrological data. It follows the formula shown below:

$$PBIAS = \left[\frac{\Sigma_{i=1}^{n}\left(Y_i^{obs} - Y_i^{sim}\right)*(100)}{\Sigma_{i=1}^{n}\left(Y_i^{obs}\right)}\right] \quad (3)$$

Where:

Y_i^{obs} is the observed streamflow.

Y_i^{sim} is the modeled streamflow.

Root mean squared error (RMSE) is a widely used measure applied to machine learning as a way of fitting the model, comparing predictions and observed data. RMSE values of 0 indicate a perfect fit between calculated and observed data. To scale and normalize this index, RMSE-observations standard deviation ratio (RSR) was chosen and has an optimal value of 0. It follows the formula shown below:

$$RSR = \frac{RMSE}{STDEV_{obs}} = \frac{\left[\sqrt{\sum_{i=1}^{n}\left(Y_i^{obs} - Y_i^{sim}\right)^2}\right]}{\left[\sqrt{\sum_{i=1}^{n}\left(Y_i^{obs} - Y^{mean}\right)^2}\right]} \quad (4)$$

Where:

Y_i^{sim} is the modeled streamflow.

Y_i^{obs} is the observed streamflow.

Y^{mean} is the mean of observed streamflow.

Unfortunately, at the time of this writing, it was not possible to retrieve the PBIAS and RSR for the SMAP and LSM models, serving only as a metric to analyze the different ANN architectures.

Analysis of variance (ANOVA) was utilized to better understand the variation between all models NSE results. ANOVA is a statistical method that compares the means of groups, in this case the different models

3 RESULTS AND DISCUSSION

The statistical values obtained for NSE for all models used are presented below in Table 3. Lower values of NSE were shown with the first run ANN model. On the first run, most values are within satisfactory range ($0.50 < NSE < 0.65$), with only a few falling below the unsatisfactory threshold. For all other models, NSE values stayed at good ($0.65 < NSE < 0.75$) or very good ($NSE > 0.75$) threshold. Validation for the calibrated data is unsatisfactory for most basins at ANN first run, with negative values. For the other ANN models, 2 out of 5 basins show unsatisfactory NSE values and 3 out of 5 shows very good NSE values.

Table 3 - NSE calibration values for all basins and each run of different ANN models, SMAP model and LSM model and the available validation results. CNN - 1 is the first ANN run, CNN - 2 is the second ANN run and CNN-SMAP is the run where the modeled SMAP streamflow was used as an input to the ANN model. Source: Author.

	CNN - 1		CNN - 2		RNN		CNN-SMAP		SMAP	LSM
Basin	**Cal**	**Val**	**Cal**	**Val**	**Cal**	**Val**	**Cal**	**Val**	**Cal**	**Cal**
A. Ver.	0,52		0,89		0,99		0,83		0,73	0,81
B. Monte	0,75	0,62	0,93	0,83	0,98	0,83	0,93	0,82	0,74	0,86
D. Franc.	0,60		0,84		0,99		0,84		0,73	0,68
Embor.	0,65		0,87		1,00		0,82		0,78	0,77
Furnas	0,63		0,92		0,99		0,89		0,94	0,88
Itá	0,77		0,90		0,99		0,88		0,58	0,53
Itaipú	0,32		0,78		0,99		0,80		0,57	0,68
Itapebi	0,12	-0,28	0,89	0,10	0,92	0,12	0,87	0,06	0,79	0,85
Itumbiara	0,73		0,89		0,99		0,84		0,73	0,82
Lajeado	0,66		0,95		0,99		0,94		0,86	0,80
Mascar.	0,53	-0,06	0,79	0,32	0,98	0,36	0,75	0,45	0,81	0,81
N. Avan.	0,50		0,91		0,99		0,92		0,89	0,84
Nova Ponte	0,76		0,93		1,00		0,88		0,91	0,83
P. Prima.	0,72		0,90		0,99		0,85		0,75	0,76
Rosana	0,36		0,87		0,99		0,78		0,83	0,74
S. Caxias	0,70		0,86		0,98		0,87		0,65	0,61
S. Cecília	0,66		0,89		0,99		0,89		0,73	0,84
S. Antô.	0,71	-0,05	0,93	0,90	0,96	0,91	0,93	0,88	0,58	0,94
São Simão	0,74		0,94		0,99		0,88		0,87	0,90
S.Mesa	0,76		0,94		0,99		0,90		0,77	0,85
Sobrad.	0,40		0,85		0,99		0,85		0,83	0,84
T. Pires	0,47	0,03	0,92	0,71	0,97	0,83	0,91	0,78	0,83	0,89
T. Marias	0,79		0,82		1,00		0,78		0,85	0,74
Tucuruí	0,73		0,96		0,98		0,87		0,62	0,88
Xingó	0,39		0,86		1,00		0,70		0,03	0,35

PBIAS only for the ANN models are presented in Table 4. Except for two values, all PBIAS values are within the very good threshold (PBIAS < ±10). The remaining two values, located in the validation step, are within the good threshold (±10 < PBIAS < ±15).

Table 4 - PBIAS calibration values for all basins and each run of different ANN models and the available validation results. CNN - 1 is the first ANN run, CNN - 2 is the second ANN run and CNN-SMAP is the run where the modeled SMAP streamflow was used as an input to the ANN model. Source: Author.

	CNN - 1		CNN - 2		RNN		CNN-SMAP	

Basin	Cal	Val	Cal	Val	Cal	Val	Cal	Val
A. Ver.	-9,96		-0,44		-1,32		1,72	
B. Monte	3,43	1,22	-0,41	-5,78	6,43	1,68	-2,02	-5,11
D. Franc.	2,32		6,22		2,17		2,73	
Embor.	2,67		5,10		1,77		2,03	
Furnas	-3,89		4,98		0,07		-0,99	
Itá	4,30		3,20		1,33		5,04	
Itaipú	-1,17		-2,79		1,32		-0,49	
Itapebi	-2,18	1,05	6,48	3,62	1,58	-2,11	6,87	-0,46
Itumbiara	0,45		0,25		0,76		-0,99	
Lajeado	8,40		1,63		6,15		1,23	
Mascar.	6,11	2,57	-0,61	2,16	0,77	7,52	0,17	18,34
N. Avan.	-1,04		0,22		3,08		2,50	
Nova Ponte	2,82		2,68		1,81		0,19	
P. Prima.	-3,24		0,80		1,14		3,77	
Rosana	-8,90		0,52		-0,11		1,79	
S. Caxias	1,98		2,96		3,60		-0,91	
S. Cecília	1,93		1,67		2,28		-1,53	
S. Antô.	7,26	7,49	2,73	-1,98	2,57	-3,45	-3,83	-1,97
São Simão	2,68		0,45		0,33		-2,28	
S.Mesa	2,68		6,26		1,42		-0,69	
Sobrad.	2,18		-0,17		-1,38		0,66	
T. Pires	2,38	9,14	-1,84	1,34	-1,18	1,58	1,09	15,36
T. Marias	4,92		2,67		2,77		9,24	
Tucuruí	3,36		-0,83		2,74		-5,15	
Xingó	1,00		5,91		0,29		1,68	

RSR only for the ANN models are presented in Table 5. Except for some values in the calibration step of the first CNN run, all RSR calibration values are within the very good threshold (RSR < 0.50). The first CNN run RSR calibration values are within the good (0.50 < RSR < 0.60) or satisfactory (0.60 < RSR < 0.70) threshold. For the validation step, Belo Monte basin was very good, Itapebi and Masceranhas were good at the second CNN run and on the CNN-SMAP run, and unsatisfactory at the other models. Santo Antonio and Teles Pires were good at the second CNN run, RNN and CNN-SMAP run, and- unsatisfactory at the first CNN run.

Table 5 - RSR calibration values for all basins and each run of different ANN models and the available validation results. CNN - 1 is the first ANN run, CNN - 2 is the second ANN run and CNN-SMAP is the run where the modeled SMAP streamflow was used as an input to the ANN model. Source: Author.

	CNN - 1		CNN - 2		RNN		CNN-SMAP	
Basin	**Cal**	**Val**	**Cal**	**Val**	**Cal**	**Val**	**Cal**	**Val**
A. Ver.	0,54		0,23		0,09		0,30	
B. Monte	0,35	0,37	0,21	0,26	0,15	0,41	0,20	0,27
D. Franc.	0,46		0,25		0,09		0,32	
Embor.	0,45		0,27		0,07		0,30	
Furnas	0,44		0,21		0,10		0,24	
Itá	0,33		0,25		0,09		0,28	
Itaipú	0,67		0,34		0,11		0,36	
Itapebi	0,65	0,80	0,21	0,55	0,29	0,94	0,23	0,60
Itumbiara	0,40		0,25		0,09		0,31	
Lajeado	0,40		0,17		0,12		0,18	
Mascar.	0,47	0,69	0,34	0,51	0,15	0,80	0,33	0,47
N. Avan.	0,51		0,22		0,08		0,22	
Nova Ponte	0,37		0,18		0,07		0,27	
P. Prima.	0,42		0,23		0,10		0,30	
Rosana	0,59		0,27		0,09		0,35	
S. Caxias	0,40		0,29		0,13		0,29	
S. Cecília	0,46		0,23		0,12		0,25	
S. Antô.	0,41	0,62	0,19	0,23	0,20	0.31	0,20	0,26
São Simão	0,39		0,18		0,10		0,27	
S.Mesa	0,38		0,19		0,07		0,24	
Sobrad.	0,55		0,29		0,10		0,30	
T. Pires	0,53	0,59	0,22	0,34	0,17	0,41	0,22	0,32
T. Marias	0,33		0,27		0,06		0,30	
Tucuruí	0,34		0,15		0,14		0,27	
Xingó	0,51		0,24		0,07		0,31	

For computational usage, the Table 6 presents time values for each epoch to run and each RCM. Google cloud based computation was used for the study.

Table 6 - Average computational time for each ANN model. Source: Author.

Model	**Average time per epoch (ms)**	**Average epoch amount (steps)**	**Average time (min)**	**Total training time (min)**
CNN - 1	14	1532	0,36	8,94
CNN - 2	14	1752	0,41	10,22
RNN	49	2779	2,27	56,74
CNN-SMAP	17	2983	0,85	21,13

A summary statistics of the streamflo modeled data is shown in Table 7 below.

Table 7 - Minimum, maximum, median and mean values for all basins for different models. Source: Author.

	CNN.1.Run	CNN.2.Run	RNN	SMAP.run	SMAP	MEL
Água Vermelha						
Min.	832,04	573,89	512,08	589,95	267,98	298,00
1st Qu.	1120,97	1411,29	848,86	1244,37	755,14	588,75
Median	1307,36	2190,56	947,47	1871,63	1096,25	774,00
Mean	1541,02	2096,37	1099,93	1945,95	1346,07	897,38
3rd Qu.	1801,72	2784,38	1117,80	2682,26	1688,62	1150,25
Max.	3267,92	3271,32	3190,22	3269,92	8289,17	3023,00
Belo Monte						
Min.	1580,33	1546,06	2894,77	1460,34	545,86	630,00
1st Qu.	13493,23	9777,93	5025,96	6616,34	1447,88	2313,75
Median	14540,63	15276,46	6909,08	11754,37	2511,31	3890,50
Mean	13133,52	13553,54	9034,84	11261,59	4179,98	4644,48
3rd Qu.	15513,44	18078,28	11815,79	15725,57	5243,68	6376,25
Max.	17322,22	21382,03	21666,28	21598,43	33876,94	20949,00
Dona Francisca						
Min.	79,84	74,56	73,34	75,64	37,27	81,00
1st Qu.	228,89	203,96	293,28	210,29	106,36	169,00
Median	394,82	475,28	590,77	416,73	162,38	238,00
Mean	449,79	646,16	818,52	536,77	216,64	255,77
3rd Qu.	581,57	1070,69	1442,52	793,68	273,97	325,00
Max.	1650,59	1890,44	1950,22	1855,33	1379,34	850,00
Emborcação						
Min.	246,92	216,26	239,51	240,01	56,29	44,00
1st Qu.	551,05	401,10	415,86	395,22	148,83	134,00
Median	636,13	490,99	558,35	499,48	230,76	172,00
Mean	643,61	532,62	565,21	555,66	307,15	217,40
3rd Qu.	746,87	631,71	719,53	691,89	381,56	273,00
Max.	1012,72	1066,26	1076,02	1084,91	2342,07	1036,00
Furnas						
Min.	495,97	391,15	338,63	334,92	137,49	128,00
1st Qu.	693,05	664,95	422,95	539,44	485,03	340,00
Median	814,88	1098,06	516,65	893,94	759,68	469,00
Mean	994,18	1477,20	631,91	1283,58	908,44	573,21
3rd Qu.	1144,35	2278,99	728,94	1905,23	1191,94	769,00
Max.	3064,87	3554,39	2942,83	3589,87	4987,44	2110,00

			Itá			
Min.	311,65	272,10	378,10	301,05	78,09	128,00
1st Qu.	584,59	551,86	600,76	561,48	474,78	551,00
Median	1087,19	1554,66	1519,17	1883,60	793,33	846,00
Mean	1363,07	1834,17	1796,87	2091,59	1023,90	950,44
3rd Qu.	1890,67	3004,57	2774,66	3595,10	1327,58	1229,00
Max.	4407,30	4563,71	4596,52	4596,60	7536,45	3745,00
			Itaipu			
Min.	4729,17	3333,14	3007,83	3044,65	499,72	1335,00
1st Qu.	4932,20	3821,74	3415,21	3347,82	1713,20	1723,00
Median	5082,24	4163,48	3942,22	3537,20	2263,81	2168,00
Mean	5374,28	4509,64	4397,31	3729,80	2472,89	2455,29
3rd Qu.	5385,30	4816,84	5195,19	3881,91	3004,11	2850,00
Max.	12783,69	12563,09	13178,94	10361,56	11559,00	10701,00
			Itapebi			
Min.	72,88	73,26	41,91	68,10	36,08	32,00
1st Qu.	75,36	185,17	181,38	323,67	119,00	47,00
Median	79,52	286,60	446,73	448,93	219,78	80,00
Mean	83,44	381,32	429,48	569,88	451,35	157,35
3rd Qu.	85,51	417,01	636,21	708,68	558,56	221,00
Max.	204,89	1561,72	1588,44	1591,91	4435,57	1024,00
			Itumbiara			
Min.	362,98	343,82	305,68	332,60	144,92	140,00
1st Qu.	788,92	603,59	639,18	466,38	338,33	261,00
Median	968,40	782,06	834,18	584,76	501,13	353,00
Mean	953,99	825,12	859,17	708,58	639,85	428,90
3rd Qu.	1121,17	1033,55	1000,02	930,66	824,84	563,00
Max.	1526,96	1519,39	1564,82	1527,33	3674,43	1474,00
			Lajeado			
Min.	779,61	388,67	304,03	361,42	185,33	108,00
1st Qu.	2522,84	908,65	306,15	406,14	485,64	438,00
Median	3333,59	1341,53	318,08	484,45	816,20	589,00
Mean	3203,45	1809,74	694,11	901,55	1327,45	825,07
3rd Qu.	3905,79	2402,48	475,94	771,44	1577,10	1092,00
Max.	5381,57	5450,93	5463,15	5515,85	13132,59	4180,00
			Mascarenhas			
Min.	303,69	301,34	244,28	323,78	146,07	186,00
1st Qu.	623,86	348,07	266,20	374,47	403,48	273,00
Median	710,61	409,24	431,01	449,61	681,15	409,00

Mean	728,41	672,67	763,24	716,82	1050,16	594,09
3rd Qu.	817,95	784,95	1115,52	878,32	1295,48	796,25
Max.	1350,46	2335,11	2339,35	2361,23	13034,02	3172,00
			Nova Avanhandava			
Min.	501,31	447,49	447,58	448,93	182,75	276,00
1st Qu.	624,44	663,68	812,55	633,41	443,96	440,00
Median	701,69	861,64	833,78	841,47	642,48	551,00
Mean	783,03	1023,08	884,70	1050,43	759,73	622,76
3rd Qu.	871,34	1266,64	931,96	1372,23	945,50	777,00
Max.	2253,74	2471,03	2359,16	2493,75	4889,69	1939,00
			Nova Ponte			
Min.	159,99	125,20	125,96	114,13	42,72	46,00
1st Qu.	227,69	228,88	165,84	185,59	120,26	117,00
Median	260,32	310,38	191,19	251,25	185,62	146,00
Mean	328,50	379,53	230,37	337,18	233,71	184,53
3rd Qu.	338,79	484,62	254,00	440,77	299,33	236,00
Max.	1025,23	1024,21	1000,51	1028,10	1702,03	731,00
			Porto Primavera			
Min.	2708,28	2206,45	2289,18	2113,82	758,91	822,00
1st Qu.	3416,08	2706,62	2937,98	2378,04	1638,20	1321,00
Median	3628,14	3160,59	3028,72	2623,99	2095,40	1673,00
Mean	3852,06	3561,12	3221,36	2922,57	2312,79	1821,05
3rd Qu.	4012,79	4069,91	3299,86	3137,89	2771,28	2200,00
Max.	8523,53	8550,42	8512,54	8267,42	9123,06	5805,00
			Rosana			
Min.	1060,98	831,01	935,68	815,92	421,13	671,00
1st Qu.	1225,09	1265,14	1626,73	1306,81	1100,18	918,00
Median	1333,59	1745,19	1877,50	1865,41	1499,69	1179,00
Mean	1519,24	2026,54	2039,66	2105,22	1658,69	1275,91
3rd Qu.	1597,26	2573,02	2413,49	2727,84	2030,08	1556,00
Max.	4233,60	4774,38	4328,06	4731,62	6730,69	4159,00
			Salto de Caxias			
Min.	759,29	639,64	694,85	721,42	84,27	398,00
1st Qu.	1180,17	1019,20	1073,99	1116,65	770,63	997,00
Median	1630,37	1697,71	1578,90	2155,47	1190,08	1440,00
Mean	2154,49	2161,58	1860,03	2453,26	1393,97	1561,48
3rd Qu.	2960,71	3095,00	2282,19	3617,94	1801,08	2015,00
Max.	5825,23	5883,56	5803,35	5959,83	8852,56	5350,00

Santa Cecília						
Min.	168,60	137,48	132,38	126,83	44,50	89,00
1st Qu.	228,95	149,01	132,45	131,31	119,54	116,00
Median	270,36	156,51	132,70	134,47	165,13	140,00
Mean	283,43	164,89	134,29	137,85	178,07	162,44
3rd Qu.	316,24	171,00	133,83	140,13	222,73	201,00
Max.	623,64	404,93	293,22	297,43	634,72	435,00
Santo Antônio						
Min.	13733,79	11573,63	4101,74	7232,19	4011,18	2089,00
1st Qu.	28835,28	19647,01	7071,04	11008,83	10204,28	9629,75
Median	31002,75	23746,53	10221,78	14712,81	14263,10	14592,00
Mean	30068,09	24266,06	14271,83	18407,99	17007,74	15638,18
3rd Qu.	32005,83	28901,22	20567,94	24937,00	21465,27	20494,75
Max.	36813,48	37882,92	37825,26	40214,32	70905,65	50719,00
São Simão						
Min.	1043,60	999,54	667,34	877,20	299,76	254,00
1st Qu.	1646,58	1767,01	732,09	1424,14	583,05	483,00
Median	1892,81	2367,84	1039,22	1958,88	763,31	569,00
Mean	2043,14	2446,22	1424,75	2097,49	881,46	670,19
3rd Qu.	2271,05	3092,75	1767,24	2680,54	1058,77	804,00
Max.	4124,07	4353,22	4481,57	4350,70	4379,79	3022,00
Serra da Mesa						
Min.	200,89	143,07	145,63	133,54	92,01	69,00
1st Qu.	547,04	175,89	147,66	154,96	223,94	143,00
Median	918,42	299,70	150,19	193,04	401,48	307,00
Mean	1076,27	610,79	155,20	404,68	656,93	399,35
3rd Qu.	1677,60	939,81	153,26	375,47	868,62	578,00
Max.	2100,39	2138,21	1621,13	2188,30	5892,82	2142,00
Sobradinho						
Min.	1088,65	519,30	-1,99	319,69	562,94	362,00
1st Qu.	1240,66	1032,61	515,02	1181,10	2838,87	546,00
Median	1321,51	1365,76	763,95	1457,54	4313,65	596,00
Mean	1381,59	1392,91	927,30	1481,75	5112,04	899,41
3rd Qu.	1510,49	1793,22	1347,97	1821,52	6397,65	1114,00
Max.	1889,34	2098,32	2039,30	2120,51	26401,61	4114,00
Teles Pires						
Min.	1786,04	1332,11	1646,84	1012,11	324,02	373,00
1st Qu.	3456,57	2867,06	2509,58	1655,57	633,56	814,00
Median	4095,82	3463,47	2850,20	1982,73	837,26	871,00

Mean	3763,10	3328,74	3035,45	2189,84	1022,75	1084,97
3rd Qu.	4241,90	3799,03	3356,36	2436,60	1200,79	1280,25
Max.	4416,29	5192,22	5264,84	5189,15	4901,98	3991,00
			Três Marias			
Min.	277,24	371,17	279,01	362,65	94,11	52,00
1st Qu.	696,81	1486,76	361,53	973,22	289,97	215,00
Median	2962,25	2387,53	429,68	1390,73	487,14	271,00
Mean	2269,32	2185,76	587,20	1622,35	655,67	385,63
3rd Qu.	3398,75	2852,19	678,44	2242,64	854,54	514,00
Max.	3501,87	3479,06	3474,60	3457,79	5209,10	1847,00
			Tucuruí			
Min.	3032,53	2353,90	1641,80	2834,28	923,46	739,00
1st Qu.	9954,91	5263,09	1684,12	6171,62	2441,28	2800,75
Median	14686,73	11268,18	1704,80	10714,08	3915,03	4459,50
Mean	16152,73	13807,28	2198,54	12477,01	6364,67	6159,63
3rd Qu.	24265,57	22786,36	1770,11	16709,37	7982,60	8029,75
Max.	27516,71	30848,45	27121,91	32040,22	59044,46	27228,00
			Xingó			
Min.	480,98	259,30	314,27	247,62	4,90	0,00
1st Qu.	483,81	261,04	323,71	248,97	33,34	2,00
Median	496,51	263,77	324,79	251,71	103,25	10,00
Mean	751,44	282,25	330,81	273,15	560,42	46,19
3rd Qu.	637,97	277,88	327,40	263,47	612,13	52,00
Max.	4504,43	1360,12	4972,12	4044,85	8364,25	1304,00

With the preliminary statistical analysis done, specific methods were implemented for continued performance evaluation. First, the streamflows were normalized according to the historical climate normal from 1960 to 1989, in an attempt to better encapsulate what are the future trends that the models display. This normalization was executed by averaging the streamflow values of every individual month on the different models and dividing it by the equivalent month of the historical climate normal. After careful consideration, Sobradinho was omitted from the graphical analysis, since SMAP had widely different streamflow when compared with all other tools The first CNN run had the same issue with Três Marias for the June-July-August (JJA) period, so it was also omitted for the JJA figure. The climate model Eta-BESM 8.5 was the most extreme scenario analyzed, as shown in Figure 3 below. All other climate models have similar behavior.

Figure 3 - Modeled data normalized with historical climate normal (1960 to 1989)

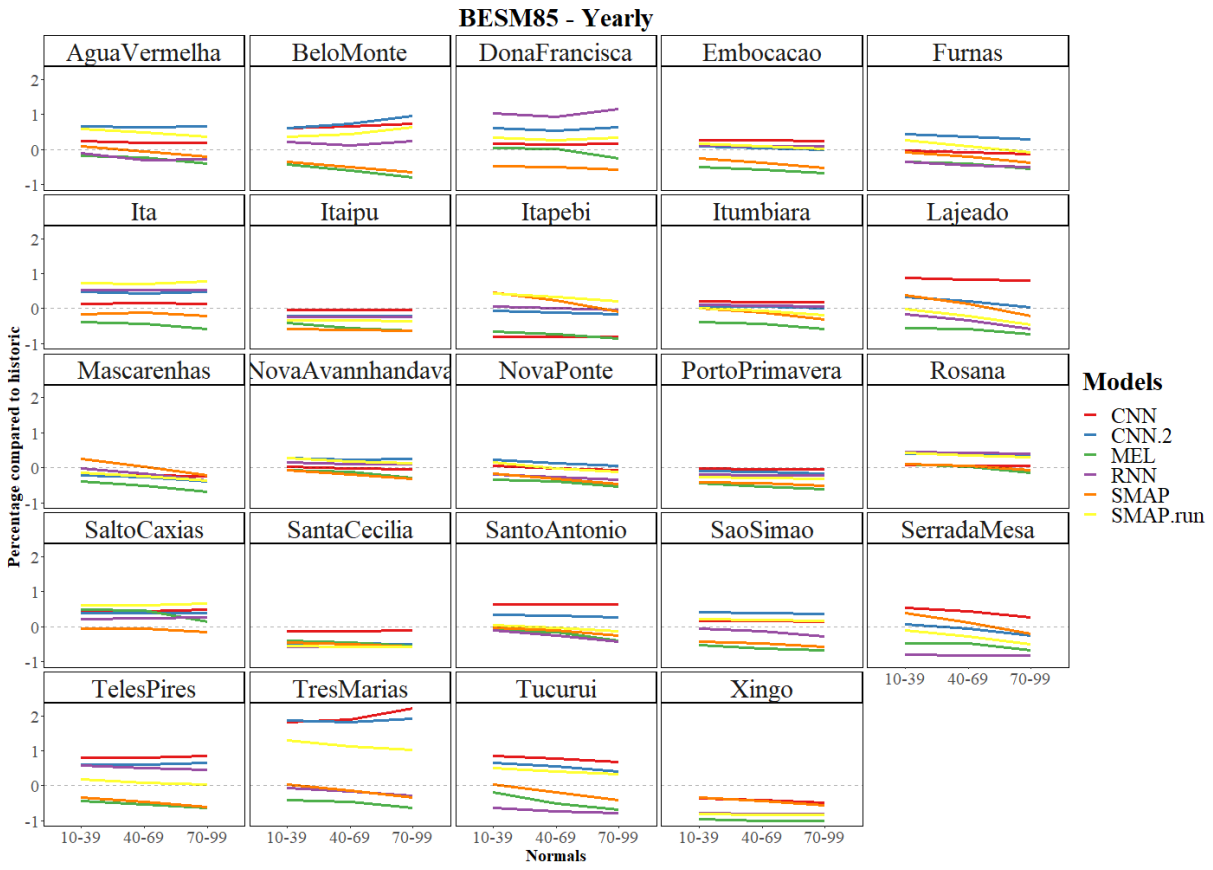

Source: Author (2023).

This data can also be parceled into different seasons, to better evaluate gains and losses in the dry and rainy season. The two seasons evaluated were JJA and December-January-February (DJF) in accordance with Chou et al. (2014) paper, presented in Figures 4 and 5 below.

Figure 4 - Modeled data normalized with historical climate normal (1960 to 1989) for the season of DJF

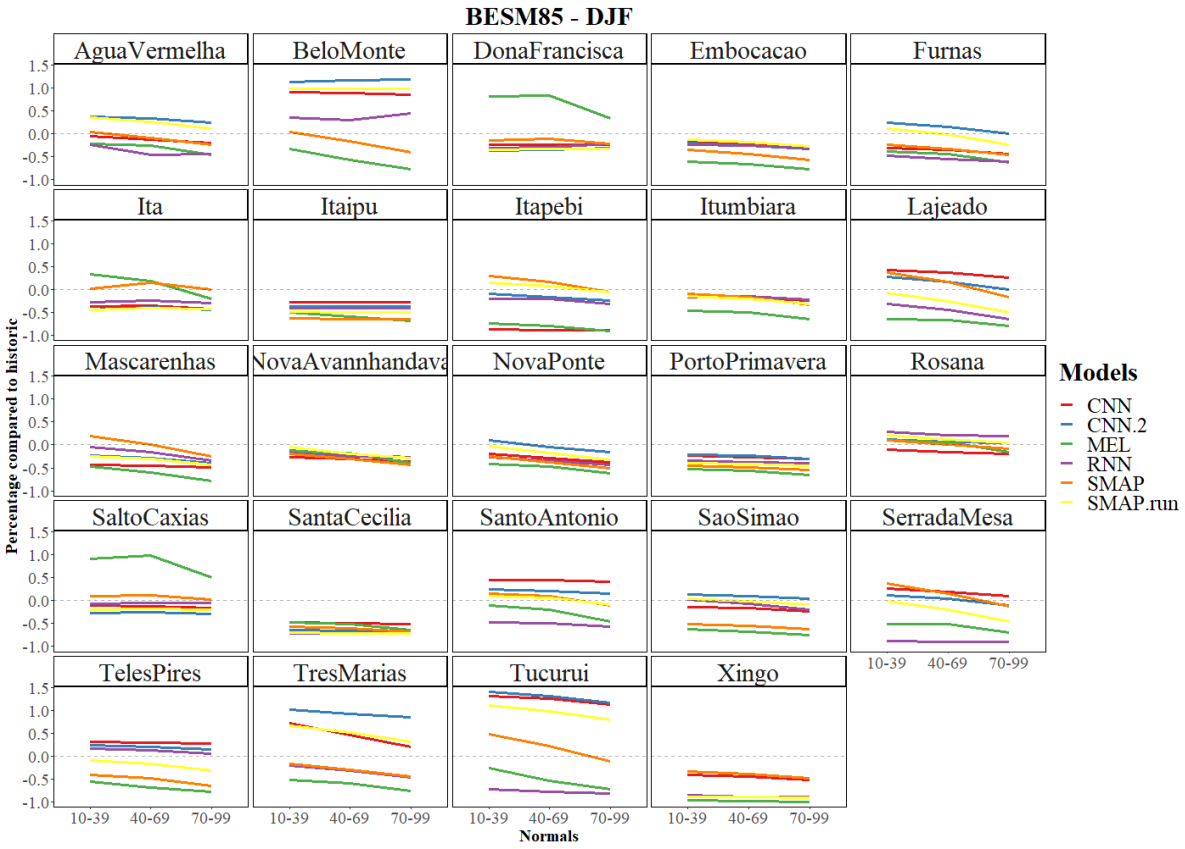

Source: Author (2023).

Figure 5 - Modeled data normalized with historical climate normal (1960 to 1989) for the season of JJA

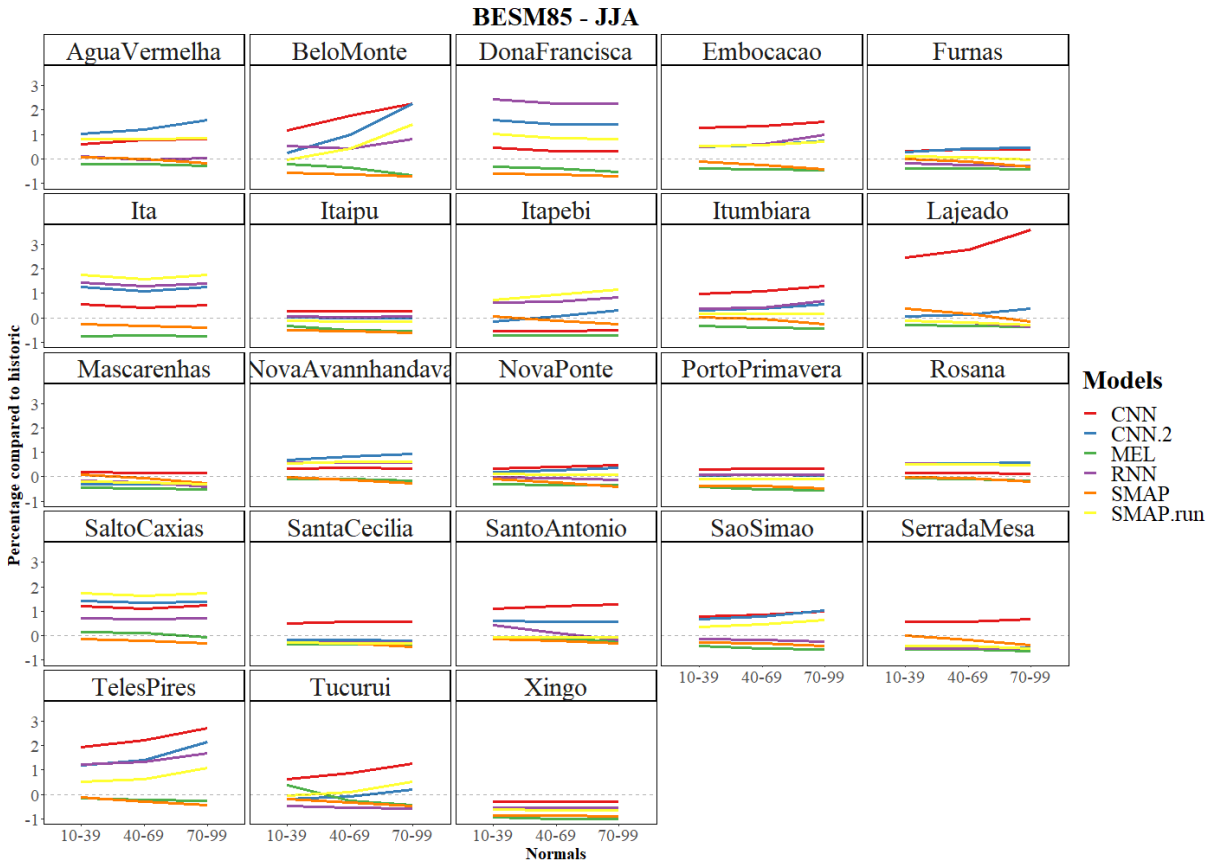

Source: Author (2023).

After that, a dimensionality reduction through UMAP was executed, generating the Figure 6 below.

Figure 6 - Dimensionality reduction through UMAP of streamflow for all models and climate models

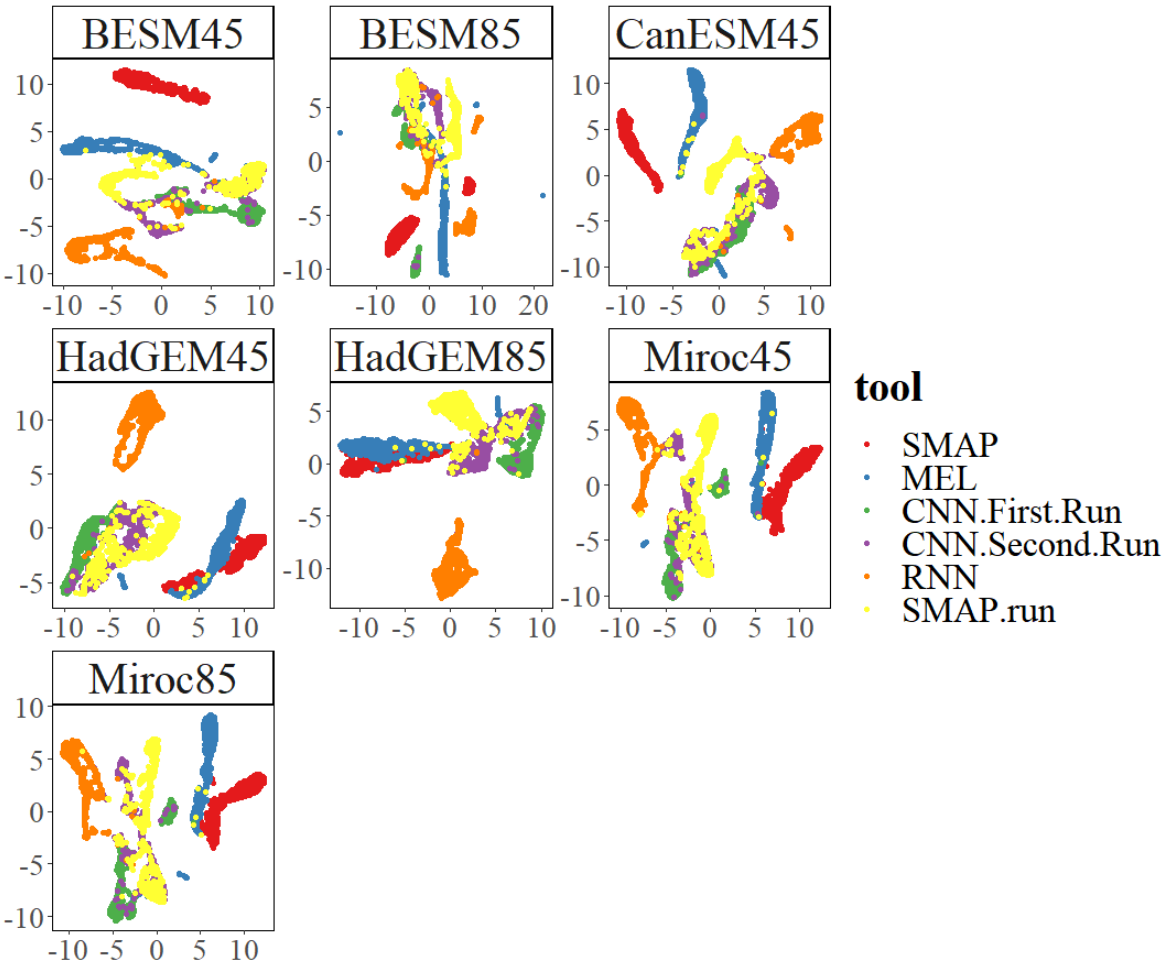

Source: Author (2023).

By comparing the improvement between calibration and validation, we can argue that the data sizes were sufficient for calibration, but suffered with the smaller validation size. A bigger dataset is suggested for further studies with special attention to bigger datasets for calibration. Since the neural network can only learn from available data, the maximums and minimums of the historical set are the constraints for the maximum and minimum values for the predicted data. That does not represent reality, since extreme events of drought and rainfall that surpass historical values can occur. When analyzing the maximum and minimum values for all models, it is clear that the ANN models struggle with minimum streamflow values, having a higher minimum when compared to the mainstream tools in all bains except Sobradinho. This makes the average streamflow higher than the compared SMAP and MEL models. Still, an ANOVA analysis of all models reveals that all models have different means (p value < 0.0001), with very few exceptions that can be further investigated. With a bigger

dataset, the ANN can learn with past extreme historical events, although this constraint still remains in some form. Additionally, a bigger dataset could be split into a training and testing set, reducing the overfit problem presented. A bigger validation set is also recommended, to better evaluate the statistical indexes.

The ANOVA shows that all NSE but the SMAP and MEL (p-value = 0.32) are statistically significantly different (p-value < 0.016). This shows that the ANN models are sensitive to alterations in input data and, even if the input is still the same, the architecture plays a role on the final NSE value. On top of that, the first CNN run shows the greatest NSE variance, while the second CNN run, RNN and CNN-SMAP were much more consistent in learning the data.

The negative values of PBIAS makes sense considering the ANN environment. ANN architectures can easily overfit the data and lead to overestimation biases. However, reducing the training time can also lead to gross underestimation. To correct, it is suggested to fine tune the hyperparameters inside the neural network architecture, and further investigate the robustness of the same architectures when recompiling multiple times, as the current study was faced with difference between consecutives recompiles. An issue noticed throughout the many recompiles conducted in this study was that even by setting a seed for the random number generators the ANNs output still varied. A potential solution for this problem is increasing the amount of features artificially or adding the SMAP output, as noted by the improvement of the CNN-SMAP run and second CNN run when compared to the first CNN run. Another solution could be adding more features, including more monthly, doing it with daily precipitation data, temperature, wind and irradiation, although the latter can be hard to find for most basins in Brazil. Another solution could be using pre-trained neural networks, which can also help with the limited amount of data available.

The computational times revealed that the RNN training time for all basins can take up to an hour, not considering time between basins and other Google Cloud related limitations, giving an edge to the CNN based runs, since they only take 20 minutes maximum to train for all basins. Still, with the present study it is recommended to run both the RNN and CNN, either second CNN run or CNN-SMAP run, until further studies can settle between one or the other.

When the historical and predicted data are compared, it is clear the similarities between the second CNN run and CNN-SMAP run. The statistical analysis shown previously reflects these similarities, with great overlap between the two runs in UMAP and similar NSE, PBIAS and RSR values. For the RNN run, this model has been statistically sound, often with

the highest NSE, PBIAS and RSR scores, and with low overestimation bias. However, it is well known that all hydrological analysis should also include visual analysis of the hydrograms on top of statistical analysis.

Overall, running the CNN a second time with the outputs produced by the first CNN run improved the NSE results for calibration and evaluation across the board. PBIAS showed a tendency of the second CNN run to overfit the data while RSR was also improved across the board. With that, the second CNN run is better at learning the input data and its labels, but that can lead to overestimation when predicting future streamflow.

The predicted-historical comparative graph reveals that although the Eta-BESM 8.5 is the most extreme case when it comes to losses in streamflow, other models differ a little depending on the basin analyzed. Some even present gains over the climate normals, and introduce a complexity, which is not the focus of this study. Overall, the ANN models agree with the mainstream models (SMAP and LSM).

The UMAP dimensionality reduction analysis provides a visual aid to evaluate how similar and distinct the different models are. It is important to note that distance between clusters do not mean anything per se, but overlap between clusters do. With that, it becomes clear that CNN-SMAP model is an “in between” when comparing all the different models. The ANN models tend to cluster together, and the same happens with the MEL and SMAP model. The CNN-SMAP model could lead to improved predictions, with the known reliability of SMAP predictions and the statistical consistency with learning the historical data of the ANN models. Another fact is that any tool has weaknesses and strengths by itself, and by comparing the results between them we can have an improved understanding of predicted values. This is already true, as most hydrologists do a weighted approach to SMAP and LSM results, using 50% of each tool to get a refined result for long term predictions. This gives the CNN-SMAP an edge, as it takes two tools in consideration.

When the hydrograms were evaluated, it was noted that overestimation bias was occurring on the second CNN run and RNN run. Although statistically similar, graphical differences started to appear when the neural networks were requested to predict future climate behavior with the 2010-2099 rainfall and evapotranspiration data. Overall, except the first CNN run, where the model did not have enough input information to learn the data correctly, all ANN models were able to learn the historical data well, and were able to predict reliable results for almost all basins and models. Only one basin, Sobradinho, showed a great difference between the SMAP models and all other models. For this basin, the input data where the ANN learned the behavior of streamflow ranged from -1,99, or 0 as the negative

value is an artifact of the RNN model, to 2120,52, where the SMAP models generated results from 562,94 to 26401,61. Even the LSM model only generated data from 362 to 4114. This difference can be further investigated, as the same historical data was used in all models and still generated widely different results.

4 CONCLUSION

The present study was successful in developing an ANN from scratch to obtain future simulated data. Many challenges and difficulties arise from this study, opening the path for future studies.

A difficulty with using the same architecture for different basins is that they have different hydrological behaviors and the ANN could benefit if there was some hyperparameter tuning for each basin, although it would bring another level of complexity to the user. Automatic sweeps across possible hyperparameters could present a computational challenge.

A next step, after increasing the model robustness further, would be to build a website to encapsulate the ANN, where it would automatically generate the results of streamflow, based on the user input file. The input files could be the readily available files given by the National Conjuncture of Brazilian Water Resources (ANA) and CPTEC/INPE.

A proposed study would be to investigate similar basins and basins that have sinusoid-like streamflows, with low occurrences of extreme events between years. These basins might have reservoirs that normalize the streamflow and can negatively affect ANN based models, since they recognize patterns and apply to all future predictions. An example of this basin could be Nova Ponte. Also, clustering basins by regions would also be advised, since different climatic zones are acting, with their own particularities.

REFERENCES

CHOU, S. C., *et al*. Assessment of climate change over South America under RCP 4.5 and 8.5 downscaling scenarios. **American Journal of Climate Change**, 3(5), 512-527, [*s. l.*], 2014.

INTERNATIONAL PANEL FOR CLIMATE CHANGE. Climate change 2013: The physical science basis. Contribution of working group I to the Fifth Assessment Report of the Intergovernmental Panel on Climate Change. **Cambridge University Press**, [*s. l.*], 2013.

CHOU, S. C., *et al*. Assessment of climate change over South America under RCP 4.5 and 8.5 downscaling scenarios using the Eta regional climate model. **Theoretical and Applied Climatology**, 117(1-2), 49-65, [*s. l.*], 2014.

CHOU, C., *et al*. Downscaling of South America present climate driven by 4-member HadCM3 runs. **Climate Dynamics**, 42(11-12), 3213-3232, [*s. l.*], 2014.

COLLINS, M. *et al*. (2021). Challenges and opportunities for improved understanding of regional climate dynamics. **Nature Climate Change**, 11(2), 94-101, [*s. l.*], 2021.

FLATO, G. *et al*. Evaluation of climate models. In climate change 2013: The physical science basis. Contribution of working group I to the Fifth Assessment Report of the Intergovernmental Panel on Climate Change (pp. 741-866). **Cambridge University Press**, [*s. l.*], 2013.

DUAN, Q., SOROOSHIAN, S. and GUPTA, V.K. Effective and efficient global optimization for conceptual rainfall-runoff models. **Water resources research**, 28(4), pp.1015-1031, [*s. l.*], 1992.

XU, C.Y., 1999. From GCMs to river flow: A review of downscaling methods and hydrologic modeling approaches. **Progress in Physical Geography**, 23(2), pp.229-249, [*s. l.*], 1999.

MARR, Bernard. Artificial intelligence in practice: How 50 successful companies used AI and machine learning to solve problems. **John Wiley & Sons**, [*s. l.*], 2019.

CUI, H., *et al*. Spatiotemporal variability of hydrological processes in a highly regulated river basin: A hybrid approach combining SWAT model and signal decomposition. **Journal of Hydrology**, 541b, pp.1221-1240, [*s. l.*], 2016.

DUCHI, J., HAZAN, E., & STINGER, Y. (2011). Adaptive subgradient methods for online learning and stochastic optimization. **Journal of Machine Learning Research**, 2121-2159, [*s. l.*], 2011.

FISCHER, T., & KRAUSS, C. Deep learning with long short-term memory networks for financial market predictions. **European Journal of Operational Research**, 270(2), 654-669, [*s. l.*], 2018.

LECUN, Y., BENGIO, Y., & HINTON, G. Deep learning. **Nature**, 521(7553), 436-444, [*s. l.*], 2015.

LIPTON, Z. C., BERKOWITZ, J., & ELKAN, C. A critical review of recurrent neural networks for sequence learning. [*S. l.*], 2015.

MITCHELL, T. Machine learning. **McGraw Hill**, [*s. l.*], 1997.

MUNIR K., *et al.* Cancer diagnosis using deep learning: A bibliographic review. **Cancers. Basel**, [*s. l.*], 2019.

EYRING, V. *et al.* Overview of the coupled model intercomparison Project Phase 6 (CMIP6) experimental design and organization. **Geosci. Model Dev.**, 9, 1937–1958, [*s. l.*], 2016.

COLLINS, W. J., *et al*. (2013). Long-term climate change: projections, commitments and irreversibility. In climate change 2013: The physical science basis. Contribution of working group I to the Fifth Assessment Report of the Intergovernmental Panel on Climate Change, **Cambridge University Press**, (pp. 1029-1136), [*s. l.*], 2013.

KRATZERT, F., *et al*. Towards learning universal, regional, and local hydrological behaviors via machine learning applied to large-sample datasets. **Water Resources Research**, 54(11), 8793-8815, [*s. l.*], 2018.

MIKOLOV, T., *et al*. Distributed representations of words and phrases and their compositionality. **Advances in neural information processing systems**, (pp. 3111-3119), [*s. l.*], 2013.

INTERGOVERNMENTAL PANEL FOR CLIMATE CHANGE. (2014). Climate change 2014: Synthesis report. Contribution of working groups I, II and III to the Fifth Assessment Report of the Intergovernmental Panel on Climate Change. **Cambridge University Press**, [*s. l.*], 2014.

VAN VUUREN, D. P., *et al*. The representative concentration pathways: an overview. **Climatic change**, 109(1-2), 5-31, [*s. l.*], 2011.

CHRISTENSEN, J. H., *et al*. Regional climate projections. In climate change 2007: The physical science basis. Contribution of working group I to the Fourth Assessment Report of the Intergovernmental Panel on Climate Change (pp. 847-940). **Cambridge University Press**, [*s. l.*], 2007.

MEDINA, V., *et al*. 2021. Fast physically-based model for rainfall-induced landslide susceptibility assessment at regional scale. **Catena**, [*s. l.*], 2021.

KRATZERT, F., *et al*. (2018). Towards learning universal, regional, and local hydrological behaviors via machine learning applied to large-sample datasets. **Water Resources Research**, 54(11), 8793-8815, [*s. l.*], 2018.

OLIVA, R. Model calibration as a testing strategy for system dynamics models. **European Journal of Operational Research**, 151 (3): 552–68, [*s. l.*], 2003.

VASWANI, A., *et al*. Attention is all you need. **Advances in neural information processing systems**, (pp. 5998-6008), [*s. l.*], 2017.

SAHOO, B.B., *et al*. Long short-term memory (LSTM) recurrent neural network for low-flow hydrological time series forecasting. **Acta Geophys.**, 67, 1471–148, [*s. l.*], 2019.

CHEN T. T., LEE, S. J. A weighted LS-SVM based learning system for time series forecasting, **Information Sciences**, Volume 299, Pages 99-116, [*s. l.*], 2015.

WANG, J., WANG, X., KHU, S. T. A Decomposition-based multi-model and multi-parameter ensemble forecast framework for monthly streamflow forecasting. **Journal of Hydrology**, Volume 618, 129083, [*s. l.*], 2023.

WANG, J., *et al.* Teleconnection analysis of monthly streamflow using ensemble empirical mode decomposition. **Journal of Hydrology**, Volume 582, 124411, [*s. l.*], 2020.

BECHT, E., *et al*. Dimensionality reduction for visualizing single-cell data using UMAP. **Nature biotechnology**, 37(1), 38–44, [*s. l.*], 2019.

MCINNES, L., *et al*. UMAP: Uniform manifold approximation and projection for dimension reduction. [*S. l.*], 2018.

TIEZZI, R. O., *et al*. Impacts of climate change on hydroelectric power generation – A case study focused in the Paranapanema Basin, Brazil. **Journal of Sustainable Development in Africa**, *11*(1), 140, [*s. l.*], 2018.

TIEZZI, R. O., *et al*. (2019). Trends of streamflow under climate change for 26 Brazilian basins, Brazil. **Water Policy**, *21*, 206-220, [*s. l.*], 2019.

3 CONSIDERAÇÕES FINAIS

Mudanças no clima afetam a disponibilidade de chuva e vazão dos rios. Em Chavantes e Jurumirim, as predições mostram uma redução na vazão por diversos fatores como aumento da população, mudanças no uso do solo, impermeabilização e aumento do uso de pivôs agrícolas. Por si só, esse fatores já podem ser considerados como uma ameaça para a bacia hidrográfica. Quando combinados com os impactos das mudanças climáticas, a escassez de água intensifica, impactando todas as bacias conectadas a esse bacia hidrográfica de cabeceira.

Outra ferramenta proposta é a utilização de inteligência artificial para complementar o arsenal de predição climática. A ferramenta construída foi eficaz na predição das vazões, porém muitas questões e futuros estudos surgiram. Hiperparâmetros das rede neurais podem ser melhorados em bacias individuais, a robustez da rede neural pode ser melhorada e bacias hidrográficas que apresentam um padrão de vazão podem ser investigadas com mais afinco. Essas bacias hidrográficas podem apresentar reservatórios que normalizam a vazão dos rios, o que pode ser detrimenterio para as redes neurais.

Predições climáticas é uma ferramenta fundamental para gestores de bacias hidrográficas e será imprescindível para o manejo correto das bacias hidrográficas frente às mudanças climáticas.

REFERÊNCIAS

ALMEIDA, M. S.; PAIVA, I.; MUNIZ, A. W. M. O papel do regime internacional de mudanças climáticas na promoção de políticas domésticas de mitigação no setor de energia. RP3, **Revista de Pesquisa em Políticas Públicas,** 2017, n. 1. Disponível em: https://periodicos.unb.br/index.php/rp3/article/view/14583. Acesso em: 19 jun. 2023.

MERCEDES, S. S. P.; RICO, J. A. P.; POZZO, L. de Y. Uma revisão histórica do planejamento do setor elétrico brasileiro. **Revista USP**, n. 104, p. 13-36, 2015. Disponível em: https://www.revistas.usp.br/revusp/article/view/106750. Acesso em: 19 jun. 2023.

SABINO, Edson Ricardo Calado. **Previsão de radiação solar e temperatura ambiente voltada para auxiliar a operação de usina fotovoltaicas.** 2019. Tese (Doutorado em Tecnologias Energéticas e Nucleares) – Universidade Federal de Pernambuco, Recife, 2019.

GILL, E. J., SINGH, E. B., SINGH, E. S., Training back propagation neural networks with genetic algorithm for weather forecasting. **IEEE 8th International Symposium on Intelligent Systems and Informatics**, Subotica, Serbia, pp. 465-469, [*s. l.*], 2010.

TAYLOR, K. E., STOUFFER, R. J., & MEEHL, G. A. An overview of CMIP5 and the experiment design. **Bulletin of the American Meteorological Society**, 93(4), 485-498, [*s. l.*], 2012.

FLATO, G., *et al*. Evaluation of climate models. In climate change 2013: the physical science basis. Contribution of working group I to the Fifth Assessment Report of the Intergovernmental Panel on Climate Change (pp. 741-866). **Cambridge University Press**, [*s. l.*], 2013.

HURRELL, J. W., *et al*. The community earth system model: a framework for collaborative research. **Bulletin of the American Meteorological Society**, 94(9), 1339-1360, [*s. l.*], 2013.

FASULLO, J. T., OTTO-BLIESNERl, B. L., & STEVENSON, S. ENSO's changing influence on temperature, precipitation, and wildfire in a warming climate. **Geophysical Research Letters**, 45, 9216– 9225, [*s. l.*], 2018.

CHRISTENSEN, J. H., *et al*. Regional climate projections. In climate change 2007: The physical science basis. Contribution of working group I to the Fourth Assessment Report of the Intergovernmental Panel on Climate Change (pp. 847-940). Cambridge University Press, [*s. l.*], 2007.

PAL, J. S., *et al*. Regional climate modeling for the developing world: the ICTP RegCM4 climate model. **Environmental Modelling & Software**, 103, 138-151, [*s. l.*], 2019.

REBOITA, M. S., *et al*. (2018). Previsão climática sazonal para o Brasil obtida através de modelos climáticos globais e regional. **Revista Brasileira De Meteorologia**, 33(2), 207–224, [*s. l.*], 2018.

CAMPOS, D. O., SANTOS, J. W. B., ASSIS, P. R. Aplicação do modelo hidrológico SMAP na determinação da produção de água em uma bacia hidrográfica costeira (Application of the SMAP hydrological model to determine water production in a coastal catchment area). **Revista Brasileira de Geografia Física**, v. 11, n. 1, p. 124-138, 2018. Disponível em: https://periodicos.ufpe.br/revistas/rbgfe/article/view/234165. Acesso em: 20 jun. 2023.

FERNANDES, W. S., *et al*. (2016). Avaliação do impacto das mudanças climáticas no balanço hídrico na bacia do Óros usando os modelos de mudanças climáticas do IPCC-AR4 para o cenário A1B. **Revista AIDIS De Ingeniería Y Ciencias Ambientales**, Investigación, Desarrollo Y práctica, 9(1), 28–48, [*s. l.*], 2016.

CÂMARA, R. K. C. *et al*. Modelagem hidrológica estocástica aplicada ao Rio Tocantins para a cidade de Marabá-PA. **Revista Brasileira de Meteorologia**, v. 31, n. 1, p. 11–23, [*s. l.*], 2016.

ABDELAZIZ, S. Long-Term stochastic modeling of monthly streamflow in River Nile. **Sustainability 15**, no. 3: 2170, [*s. l.*], 2023.

WANG, F., *et al.* Development of clustered polynomial chaos expansion model for stochastic hydrological prediction. **Journal of Hydrology**, Volume 595, 126022, ISSN 0022-1694, [*s. l.*], 2021.

DARCY, H. Les Fontaines publiques de la ville de dijon. **Dalmont**, [*s. l.*], 1856.

WIGMOSTA, M. S., VAIL, L. W., & LETTENMAIER, D. P. A distributed Hydrology-vegetation model for complex terrain. **Water resources research**, 30(6), [*s. l.*],1665-1679, 1994.

WOOD, A.W., *et al*. Hydrologic implications of dynamical and statistical approaches to downscaling climate model outputs. **Climatic Change 62**, 189–216, [*s. l.*], 2004.

JACOBSON, M. Z., *et al*. 100% clean and renewable wind, water, and sunlight (WWS) all-sector energy roadmaps for 139 countries of the world. **Joule**, 5(1), 43-69, [*s. l.*], 2021.

LIMA, M.A., *et al.* Renewable energy in reducing greenhouse gas emissions: Reaching the goals of the Paris agreement in Brazil. **Environmental Development**, Volume 33, [*s. l.*], 2020.

INTERGOVERNMENTAL PANEL FOR CLIMATE CHANGE. Global warming of 1.5°C. An IPCC special report on the impacts of global warming of 1.5°C above pre-industrial levels and related global greenhouse gas emission pathways, in the context of strengthening the global response to the threat of climate change, sustainable development, and efforts to eradicate poverty. **Cambridge University Press,** [*s. l.*], 2018.

STOCKER, T. F., *et al*. IPCC, 2013: Summary for policymakers. Climate change 2013: The physical science basis. Contribution of working group I to the Fifth Assessment Report of the Intergovernmental Panel on Climate Change **Cambridge University Press**, [*s. l.*], 2013.

CREUTZIG, F., *et al*. The underestimated potential of solar energy to mitigate climate change. **Nature Energy**, 2(9), 17140, [*s. l.*], 2017.

SCHMIDT, H., *et al*. Key indicators for ambitious climate mitigation. **Environmental Research Letters**, 13(5), 054028, [*s. l.*], 2018.

CHURCH, J. A., *et al*. Sea level change. In climate change 2013: The physical science basis. Contribution of working group I to the Fifth Assessment Report of the Intergovernmental Panel on Climate Change (pp. 1137-1216). **Cambridge University Press**, [*s. l.*], 2013.

LOBELL, D. B., *et al*. The critical role of extreme heat for maize production in the United States. **Nature Climate Change**, 1(9), 18-21, [*s. l.*], 2011.

SHEFFIELD, J., & WOOD, E. F. Projected changes in drought occurrence under future global warming from multi-model, multi-scenario, IPCC AR4 simulations. **Climate Dynamics**, 31(1), 79-105, [*s. l.*], 2008.

CRAWFORD, N. H., LINSLEY, R. K. Digital simulation in hydrology: Stanford watershed model IV. Stanford, Calif: Dept. of Civil Engineering, Stanford University, [*s. l.*], 1996.

MINISTÉRIO DE MINAS E ENERGIA. **Plano Nacional de Energia 2050.** Brasil, 2020.

LOBO, L., *et al*.Código 1583–etapas preliminares para estudos de avaliação da segurança de uma barragem de terra quanto ao uso e rebaixamento do nível do reservatório para abastecimento público durante a crise hídrica. **ABES**, [*s. l.*], 2023.

SILVA, J.S.D. **Espaço de viabilidade: uma ferramenta para o desenvolvimento de novas tecnologias de energias renováveis.** Tese (Doutorado em Recursos Hídricos e Saneamento Ambiental) - Universidade Federal Rio Grande do Sul, 2021.

MARASCHIN, L.C. **Dispositivos e aspectos de qualidade na gestão inteligente de energia elétrica: uma revisão da literatura.** Tese (Bacharelado em Engenharia de Controle e Automação) - Universidade Federal de Santa Catarina, 2022.

INTERGOVERNMENTAL PANEL FOR CLIMATE CHANGE. Technical Summary. In Climate Change 2021: The Physical Science Basis. Contribution of Working Group I to the Sixth Assessment Report of the Intergovernmental Panel on Climate Change. **Cambridge University Press**, Cambridge, United Kingdom and New York, NY, USA, pp. 33-144, 2021.

PRASAD, N., KUMAR, P., MM, N. An Approach to Prediction of Precipitation Using Gini Index in SLIQ Decision Tree, **2013 4th International Conference on Intelligent Systems, Modelling and Simulation**, Bangkok, Thailand, pp. 56-60, 2013.

UNESCO. The United Nations World Water Development Report 2021: Valuing Water. **United Nations**, [*s. l.*], 2021.